Response to Review 1:

We thank the reviewer for their time and effort to evaluate and develop our study. We acknowledge the constructive criticism and comments from the reviewer and propose the following revisions. We appreciate the comments by the reviewer which have resulted in a significantly strengthened manuscript.

The original comments from the reviewer are in black and in blue are the author's responses, with blue italics to show the in-text changes. We want to point out that due to many useful comments and suggestions, the major revisions have been implemented resulting in significant changes to the manuscript, as can be seen in the document attached below.

Introduction

In my opinion, the introduction needs a more stringent train of thought to lead readers into the topic more smoothly. At the start, a broader introduction to the importance of proper ice core proxy use, and especially the relevance of this study in this wider context, would help to gain the readers' attention for this work. In this regard, L28-29, L46-50, L58-61, L67-69 are already interesting hooks, on which you could expand, so that the importance of your work is explicitly stated. I would further recommend a broader climate description of the study site, because this is something the authors rely on later during the interpretation of results (e.g. L375).

We take onboard this comment by adding an additional explanation of the interpretation of d-excess in ice cores (linked to a later comment starting L22). To expand the context and the importance of this study we propose to add the following text, which creates a stronger coherence between the introduction and the discussion on isotopic fractionation.

Introduction: *"... Decreasing SSA is predominantly the result of Ostwald Ripening, where large grains grow at the cost of smaller grains (Lifshitz and Slyozov,1961; Wagner 1961; Legegneux et al., 2004), and vapour diffusion driven by sublimation from convex surfaces, and deposition onto low energy regions (Pinzer et al., 2012; Flin and Brzoska, 2008; Sokratov and Golubev, 2009). The latter is dependent on temperature (Cabanes et al., 2002), temperature gradients between the air (Ebner et al.,2017), surface and subsurface, and wind conditions (Neumann et al., 2004; Town et at., 2008). Under natural conditions SSA decrease is driven by a combination of these processes (Pinzer and Schneebeli, 2009), each potentially modifying the isotopic composition of the snow (Ebner et al., 2017)."*

Regarding the study site, we have added some additional information about the accumulation rate and synoptic conditions at EastGRIP, while an extensive description of the meteorological conditions over the three sampling seasons has been added to the results. An overview of the results section restructuring can be found in the responses in the results section of the reviewer's comments.

"The accumulation rate is approximately 14 cm w.eq. yr−1 (Schaller et al., 2017).

Westerly winds prevail during 2017 and 2018 with a wind direction of 227◦N, while 2019 had a prevailing south westerly wind (239◦N), corresponding to opposing phases of the North Atlantic Oscillation (NAO).

Significant weather conditions such as ground fog, drifting snow and snowfall, were documented each day."

L5: The phrase 'after precipitation/deposition events' used here gives me the opportunity to point out the unclear use of either term in this manuscript. Given that you refer to surface snow, which stayed at the surface for an unknown period (L38-39), I would prefer the term 'deposition' event defined more clearly somewhere in the introduction/method section and used consistently throughout the manuscript, replacing 'precipitation'.

The term 'deposition event' is now used throughout the manuscript unless specifically referring to a precipitation. We propose to add the text below to define deposition events. We also take this opportunity to add an explanation of the influence of surface hoar and or sublimation crystal formation on the surface snow, based on SSA measurements of these deposition features from previous studies.

"The term deposition events is used to describe rapid increases in SSA, expected to be from precipitation or drifted snow. It does not explicitly include surface hoar and sublimation crystal-like grain growth at the surface, given that previous studies indicate these depositional features have an SSA value around 54 m^2 kg^{-1} using SSA of hoar frost (Dominé et al., 2009)."

To account for the possibility of deposition via surface hoar we use field observations, latent heat flux measurements and temperature gradient data when analysing the isotopic change.

L22: Since the interpretation of deuterium excess as a proxy of moisture source conditions is a key background for this study, I suggest expanding on this point of the introduction. What kind of conditions were thought to be reflected by d-excess

We have expanded on the interpretation of d-excess in ice cores and what environmental conditions control d-excess.

"The second-order parameter deuterium excess (d-excess) is defined by the deviation from the near-linear relationship between δ18O and δD due to non-equilibrium (kinetic) fractionation (d-excess = δD - 8 · δ18O), and is understood to reflect moisture source conditions (Dansgaard, 1964; Merlivat and Jouzel, 1979; Johnsen et al., 1989), snow crystal formation in clouds (Ciais and Jouzel, 1994; Sodemann et al., 2008), and changes in moisture source (Masson-Delmotte et al., 2005). …

Post-depositional processes at the surface involve additional kinetic effects adding complexity to the interpretation of d-excess (Casado et al., 2016; Hughes et al., 2021; Casado et al., 2021)."

This is followed by recent studies evidencing kinetic fractionation during sublimation, as well as the supersaturated conditions leading to hoar frost which would cause large increases in d-excess (Stenni et al., Feher et al., 2021, Hughes et al., 2021; Casado et al., 2021). The revised discussion more stringently links the results from our study to previous work.

L34: As far as I can see, this is the first time, you use SSA as an abbreviation, so that an explanation of the full term and a slightly more detailed definition would be appropriate here.

We apologise for this mistake; this sentence has now been modified to the following:

*"Snow metamorphism works to reduce the snow-air interface, which can be quantified using the parameter snow specific surface area (SSA) (Legagneux et al., 2005). SSA of a snow sample is dependent on optical grain radius and density of ice (SSA=6/rhoice*dopt) (Gallet et al., 2009)".*

L43: You use the term snow 'crystals' here. I suggest replacing it with snow 'grains', here and throughout the manuscript, because you are not specifically talking about the crystallographic term but rather the ice matrix, which is mostly composed of multi- crystal ice grains.

We agree, now 'snow crystals' has been changed to 'snow grains' throughout the text.

Methods

In section 2.5.1., the definition of a decay event is not entirely clear to me.

We add the following text to improve clarity:

"To systematically identify rapid decreases in SSA, which we use as a proxy for events of snow metamorphism after deposition (identified based on the high mean SSA values), a threshold is set using the bottom 10th percentile of SSA decreases over a two-day period. This was found to result in the most equal number of events from each sampling year compared to 1- and 3-day changes. SA decay events are defined as by the initial peak, identified by the threshold, through to the next increase in SSA (rather than decrease)."

L94-96: When did you take the samples exactly? How many were afternoon samples, and does this affect the results discussed here?

The samples were all done in the daytime, and primarily done in the morning. In the submitted paper we resampled the meteorological data to the SSA sampling time-periods to ensure consistent comparison. Moreover, the decay model and model intercomparison are now based on the exact sampling time, given that the existing models are hourly resolution.

It is slightly more complicated to include the exact sampling time when assessing the relationship between change in SSA and the absolute SSA values (Fig. 1), given that we do not want to interpolate SSA as we understand that the change will not be linear throughout the day. Instead, we propose to keep the "daily" change, and clearly state the different sampling times as limitation to the model. The corresponding description has been changed to:

"*The samples were all taken in the daytime, primarily in the morning. The meteorological data is re-sampled to the SSA sampling time-periods to ensure consistent comparison.* "

L97-98: I suggest amending the title of this section, because you are not strictly talking about the calibration of the Ice Cube device but the SSA measurements using the Ice Cube.

The section title has been changed to "*SSA measurement protocol*".

L101: is 294 kg m-3 the density averaged over all three seasons, or do the seasons differ

significantly in value?

This is an average over all seasons. Annual means and standard deviations have also been added "(2017 = 307±40 kg m^{-3}, 2018 =278±47 kg m^{-3}, 2019 = 294±50 kg m^{-3})".

L108: Did you use the identical sample for SSA and stable water isotopic measurements or neighbouring material? Depending on this, the sentence in L110 needs amending: 'sealed in a polyethylene bag' or are several bags used for one sample?

The SSA samples were subsequently measured for water isotopes composition, we apologise that this was unclear. To clarify this sentence has been added to the text:

"Individual SSA samples were put in separate bags and subsequently sampled for water isotopic composition. Thus, every day the 10 SSA samples have a corresponding isotopic composition. The resultant isotope value is the average composition over the top 2.5 cm of snow."

L135: Why did you choose the threshold 6 m s-1? If I am not mistaken, blowing snow is already an issue at 5 m s-1, so that this could be a better threshold? It could also be helpful to know how many data points are in the upper spectrum of wind speeds still considered.

We agree with hindsight that this threshold is insufficient to reduce the likelihood of surface perturbation, and to address this we now use the 10-minute data from PROMICE. It is important to note here that 209 out of the total 237 sampling days have daily maximum wind speed exceeding 5 m s^{-1} and no events had wind-speed consistently below 5 m s^{-1} (two had 5.1 m s^{-1}). In addition, snowdrift events were documented in the EastGRIP field diary and correspond to wind-speeds above 7 m s^{-1}. Several events have maximum wind-speed between 6- 7 m s^{-1}, and no snowdrift documented. Based on this analysis and observations from the literature, we define two wind categories, as briefly suggested by the reviewer in a later comment, we have added a secondary wind-speed category for comparison of SSA decay when wind-speed is <6 m s^{-1} (low-wind events), and when maximum wind-speed is between 6- 7 m s^{-1} (moderate-wind events). The following text is added to the document:

"A set of criteria are required to reduce the potential of analysing events with wind-perturbed surfaces, resulting in the removal of surface snow. In Antarctica, unconsolidated surface snow has been observed to drift at wind speeds as low as 5 m s−1 measured at 2 m height (Birnbaum et al., 2010). However, a study from Greenland documented snowdrift starting at 6 m s−1 (Christiansen, 2001), likely due to warmer temperatures allowing for the surface snow to become more bonded (Li and Pomeroy, 1997). At EastGRIP, calm conditions correspond to wind speeds from 0 –5.2 m s−1 according to field diary observations. The mean daily maximum wind speed for the three sampling seasons was 6.8 m s−1, while blowing snow was documented only when wind speeds exceeded 7 m s−1. Based on this assessment, we define two wind-speed categories for comparison of the effects of wind-speed on SSA decrease. The first includes events with wind-speed consistently below 5.2 m s−1, hereafter referred to as low-wind events, to ensure no surface perturbation. Secondly, we consider events where the maximum wind-speed is between 6 –7 m s−1, hereafter referred to as the moderate-wind events. The inclusion moderate-wind events allow an assessment of the influence of wind-speed on SSA decrease."

Two SSA decay events are below the 6ms-1 threshold, both of which are from 2018. The remaining SSA decay events, E10 and E11, have maximum values of 5.1 m s^{-1}, and 5.07 m s^{-1}, respectively and last for 3-days each.

Out of the 21 initially defined events, only 2 are below the wind-speed threshold with maximum values of 5.1 m s^{-1} in both events. We expect negligible snowdrift for these two events allowing us to confidently argue that the surface is unperturbed and isotopic change is the result of snow metamorphism. The likelihood of drifting snow during moderate-wind events is considered using the equation defined from Li and Pomeroy (1998), where the threshold wind-speed for snowdrift is defined as a function of temperature.

Following the same structure as in the original manuscript, we construct the SSA decay model with parameter values set for the two wind-regimes. We add the revised figure to this response. Intuitively, the SSA decay rate is higher for moderate-wind events (-0.53 m^2 kg^{-1} day^{-1}) compared to low-wind events (-0.41 m^2 kg^{-1} day^{-1}). As the reviewer will see later in this response, we add the results from the comparison of our data and SSA decay model to existing models from Flanner and Zender (2006) and Taillandier et al. (2007).

The wind-speed distributions for the daily maximum and 10-minute mean values are also added to the supplement. For isotopic analysis we now focus on the low-wind events alone and describe the latent heat flux and temperature gradients during the two events.

L162-164: I think that you are making an important point here. Could you clarify this sentence so that it becomes obvious why you chose -25°C and not -22°C as the boundary of your SSA decay model, given that this is where snow crystal shape changes? And maybe this is better placed in the methods section.

We agree that the temperature boundaries are clearly an interesting feature of the work. Nonetheless, due to the updated wind-speed criteria, we have ultimately removed this temperature boundary condition given that the low-temperature event coincides with high-winds.

Figure 1: Firstly, the layout of this figure does a good job at visualising the sampling procedure. Unfortunately, I cannot read the site labels and the legend in panel (a). Personally, I can recommend the open-source software QGIS for designing maps. Table 1: How is the data coverage of the AWS for the seasons 2017-2019? How many data points are missing? I think that '.2' should be amended to '0.2'. The term EC needs explanation here, as it is the first time, this is mentioned.

We thank the reviewer for the suggestion to use QGIS. We have simply replaced the map as the legend in the previous figure was not relevant to the study, but QGIS will definitely be beneficial for future work. '.2' has been changed to '0.2' and added information about the eddy-covariance tower and the measurement instruments from PROMICE to the table.

Results

When it comes to the presentation of results, certain parts of the description appear repetitive (e.g. L270-273), while major conclusions are only mentioned once and are not stated clearly

enough (e.g. L283-285). Your work is really interesting, so that I would like to see (1) a concise description of all records of relevance, (2) a step-by-step line of interpretation, in which your outcomes become more visible. At the moment, the measured results and their interpretation are often mixed and the sub-division into chapters not very clear. Moreover, the chosen language is sometimes vague, leaving out important details which allow the reader to know exactly which parameter you are talking of (e.g. L240-249). I would recommend making the descriptions as precise and specific as possible, e.g. in L87 'the specific sampling dates' would be better.

Based on the reviewers' comments, we have restructured the results to improve clarity and strengthen our arguments. The new format is broadly as follows and we have included the updated figures.

1) Description of all used datasets (time-series and basic statistics between years) has been added in the first results section. Here we look mostly at the inter-annual variability and highlight the significantly lower accumulation for 2017.

2) EOF analysis follows the meteorological description to show the relationship between the dominant modes of variance of SSA, d18O and d-excess. The three parameters, SSA, d18O and d-excess are described before presenting the EOF analysis. By moving this section, the motivation for exploring the relationship between isotopic composition and SSA later in the paper becomes clearer. Here we also add the revised accumulation data for each sampling season.

3a) Description of SSA decay events extracted by the threshold, with clear explanation that events with snowfall/fog/snow drift (from field-diary) and high wind speeds are removed from further analysis. The identification of similar decay shapes in SSA time series are then noted.

3b) The empirical model to describe the SSA decrease behaviour during periods of rapid SSA decay is described for the previously described wind-speed categories. A linear regression between dSSA and SSA for the two wind-speed categories is noted to describe the decay rate and decay constant in the decay model. Based on the reviewer's comment, we first show the mean decays for each event, and in the second panel the modelled decay. In addition, we compare the model from this study to previous models from the literature. The model from Flanner and Zender (2006) is based on theoretical grain growth, and thus we can compare the observed behaviour - and our empirical model - to their physical-based model.

4a) As previously mentioned the isotopes are measured from each SSA sample, giving us a direct comparison for analysis of SSA decay events. In the same format as the original manuscript, the isotopic changes over a single day and 2-days are documented for both the low- and moderate-wind events.

4b) We then look in more detail at the two low-wind events given that we can be more certain of minimal surface perturbation. Latent heat flux and temperature gradients during these events are presented to explain the direction of fluxes.

(If repeated, precipitation isotopic composition would be measured to determine the proportion of precipitation isotope signal in a snow sample, and thus observe the change in

isotope signal from the exact precipitation signal).

L223-224: Can you provide an estimate of the probability that the top 2.5 cm sample contains material from several precipitation events? This is one part, where a more detailed climate description upfront including accumulation event frequency would be helpful.

The reviewer is indeed here asking an interesting question. Accumulation data is now added to Fig. 2 to address this point. The accumulation data shows that all the SSA samples on the first day of each decay event contained snow from more than one deposition event, given that no daily increase exceeded 2.5 cm. The uncertainty for the accumulation measurements is up to 1 cm, and therefore we cannot confidently use these measurements to approximate the number of precipitation events in one sample of snow. In addition, based on the data presented in this paper, we cannot be certain that a precipitation layer is not subsequently removed by the wind. This is added as a limitation to this study.

To account for this, we approximate the accumulation for the low-wind events, and use the field observations to identify the conditions preceding these events. The following text to the paper:

"Both E10 and E11 had consistent clear sky conditions. We note here that E11 was preceded by significant ground fog, not snowfall, indicating that the peak value of 46 m2 kg-1 was likely the result of surface hoar, and thus, the SSA decay follows an SSA peak not caused by precipitation."

"As mentioned in Section 3.2, ground fog preceded the SSA peak in E11, corresponding to negligible accumulation. In contrast, approximately 1 cm of snow was accumulated during the day prior to E10, corresponding to observation of snowfall."

L292-293: This appears to be a sentence with crucial interpretation of your records, which I think you should expand on. I am aware that the line between results and discussion section can be drawn before or after the interpretation of results, but I would like to see a clearer structure and separation from the discussion in the context of previous research.

We agree with this suggestion and propose to firstly include these previous observations more explicitly in the introduction. By focussing on the two low-wind events and their associated fluxes, the comparison to previous studies becomes more fluid. Quantification of sublimation flux during this period can potentially be added to quantify the fractionation effect. Uncertainty regarding the 2.5 cm bulk isotope measurement would hinder this approach.

"Documentation of strong sublimation during the day and weak deposition during the night corresponds to decreases in d-excess (up to 6‰) and increases in d18O of up to 1.8‰. This observation agrees with previous observation of equilibrium fractionation during sublimation (Hughes et al., 2021; Wahl et al., 2021; Casado et al., 2021). "

L304: We may be well familiar with this, but could you give a reference to back this statement, which is the result of earlier studies?

Apologies, the references Cabanes et al. (2002, 2003), Legegneux et al. (2003, 2004), Taillandier et al. (2007) and Flanner and Zender (2006) have now been added here which

documents the decreased rate of snow metamorphism with lower temperatures.

Figure 3: In my opinion, this is the most important figure when it comes to describing SSA observations and the model performance, and it nicely highlights the rapid decay at the start of SSA decay events. For some parts of your model performance discussion, it would be helpful to see observations and model outcome in one panel, so I suggest amending the current panel layout or splitting this figure into two figures about (a) observation and (b) model performance. Furthermore, I recommend using one term, i.e. 'rapid SSA decay events' or similar, throughout the manuscript to be more specific than 'events' here. And since you point out the higher intercept for temperatures <-25°C (L198) and same regression slope (L207), I suggest adding a linear regression line to panel (a) and noting somewhere that the x-axis doesn't extend to 0.

We agree with the reviewer here and have changed the figure to show a column with observed decays for b) moderate-wind events and c) low-wind events. A second column shows the modelled outputs for these events (d) and e)).

The model evaluation section is extended to include a comparison to existing models. This enables us to determine what is 'meant to be' according to physical models and compare this to observations and our model with parameters set for low-wind and moderate-wind events. The additional comparison to the moderate-wind events allows for a general assessment of the additional influence of wind on the decay rate.

The lower row of Fig. A2. now shows two events - E2 from 2017 and E18 from 2019 - that have maximum daily wind speed of 6.26 m s^{-1} and 6.28 m s^{-1} respectively, and no observed snowdrift. Based on the drift threshold defined in Li and Pomeroy (1998), E2 has potential influence from snowdrift, but not E18 (U(10) = 7.09 m/s and 8.17 m s^{-1} for E2 and E18 respectively), which agrees with an underestimation of decrease from FZ06 compared to observation during E2. Interestingly, we get the lowest RMSE values for FZ06 and the moderate wind events. Possible explanations include the initial snow conditions and event duration, which are included in the discussion.

Figure 4: Is there a way to enhance the contrast between the thick line as mean and thinner individual records? Personally, I find it a challenge to see the thick line.

Yes of course, the plot has been changed to show the individual samples as crosses ('+').

Discussion

The discussion could benefit from a wider literature context.

The discussion has been largely rewritten and more relevant recent literature has been included in the discussion. Furthermore, changes have also been made to account for our changes in the structure of the results section and our methods related to event criteria. In this revised version of the manuscript, we first discuss the different regimes resulting from the EOF analysis, referring directly to papers such as Casado et al. (2021) where they identify the relative influence of precipitation and snow metamorphism on the isotopic signal in Antarctica.

Our approach to the decay model in the study is subsequently discussed, with a focus on the comparison to previous models. We highlight the limitations relating to the fact that the two low-wind events are from 2018 while the strong coherence between d-excess and SSA from EOF analysis is observed in 2019. We highlight that the purpose of SSA decay models to predict change in SSA of a snow sample through time is not readily applied to exposed surface snow, and that there is potentially an alternative direction for future studies to focus on the multiple mechanism of surface snow reworking, that would be useful for surface energy budget calculations using remote sensing.

The structure of the isotopic analysis has been modified for more stringent comparison of our results to expectations of isotopic change from previous studies. Some sections have been merged to be more concise.

L317-318: Here, it would be good to clarify that this is in agreement with the study Taillandier et al. (2007). Are there other studies that you could compare your approach/results to?

Of course, we develop this section based on results from the model intercomparison. This enables us to discuss our empirical model with respect to the physical based model from Flanner and Zender (2006) based on theoretical grain growth. The RMSE values in Table 2 indicate that FZ06 best predicts the decay of both low- and moderate-wind events.

L333: This sentence is actually the first time you state a causal connection between SSA and d-excess development, and I recommend including this section 4.3 earlier as part of the interpretation section.

We agree with the reviewer and follow the reformatted results structure to first discuss the results from EOF analysis. We focus on the inter-annual difference in regimes, where a very strong relationship is observed in 2019, while d18O and d-excess are decoupled, compared to the opposite relationships in 2018. Our results are compared to recent work from Casado et al., 2021, who document a similar inter-annual variability in Antarctica.

L351: It would be good to see references of earlier research on these factors, i.e. sublimation, deposition and vapour diffusion, cited here.

Of course, these references have been added to show the previous work that, specifically referring to Casado et al. (2021). In addition, we propose to add more structure to the isotopes discussion by primarily identifying the expectation of isotopic change during precipitation resulting from different processes (as mentioned in the response to the previous comment).

L372: While you identify 'initial snow metamorphism' after deposition as driver of d- excess, I think that you should be more specific and discuss the importance of deposition-free phases, here described as overcast and clear-sky conditions (Table A1), for d-excess.

This point from the reviewer is appreciated and we have added a more extensive description of conditions for the events used to assess isotopic change.

A detailed description of temperature gradients and latent heat flux data during the two low-wind SSA decay events allow us to identify the processes controlling the change in isotopic

composition. The text added in response to the comment starting L393 addresses.

L381: I understand that winter snow layers have undergone more isothermal metamorphism, which is less efficient than temperature-gradient metamorphism acting especially during spring and autumn. Therefore, I recommend rephrasing 'winter layers which are less influenced by snow metamorphism'.

We agree with the reviewer and propose the following text instead:

"Snow metamorphism is thermally activated given the dominant influence of sublimation and deposition (Cabanes et al., 2002, 2003; Legegneux et al., 2004). During winter, the temperatures are very low (<-30C) and minimal insolation reduces the diurnal near-surface snow temperature gradients, resulting in isothermal metamorphism being dominant which reduces the rate of snow metamorphism, or SSA decay, compared to temperature gradient snow metamorphism (Dadic et al., 2008)*."*

L393: Section 4.6 is a very interesting and important one. The first sentence of the second paragraph appears to be a major jump in the train of thought, which I struggle to follow. Especially, the last paragraph of the conclusion contains important findings. I wish to see the last statement (L426-428) put for discussion with the same clarity earlier in the manuscript. Then, the conclusion will become a summary.

We have explained the point in L426-428 with analysis of latent heat flux and temperature gradients corresponding to isotopic change during low-wind events. As the reviewer will see, the revised structure facilitates a more concise discussion with regard to processed driving isotopic change. The following text has been added to the discussion from which we compare our observations*:*

"Three key mechanisms are expected to drive the rapid SSA decays; 1) large grains growing at the expense of small grains (Legagneux et al., 2004; Flanner and Zender, 2006), 2) diffusion of interstitial water vapour (Ebner et al., 2017; Touzeau et al., 2018; Colbeck, 1983), 3) sublimation due to the wind ventilating the saturated pore air, known as 'wind-pumping' (Neumann and Waddington, 2004; Town et al., 2008). The dominant mechanisms can theoretically be identified by a combination of the change in isotopic composition - indicating the fractionation effect - and the LE and temperature gradient data.

In theory, mechanism 1) causes minimal change in the bulk isotopic composition of a snow layer under isothermal conditions (Ebner et al., 2017). Therefore, observations of SSA decay corresponding to negligible isotopic composition change could be explained by this mechanism. We observe no events with consistent isotopic composition throughout. In the instance of 2) interstitial diffusion, light isotopes are preferentially diffused, while the heavy isotopes will be preferentially deposited onto the cold snow grains (Ebner et al., 2017; Touzeau et al., 2018; Colbeck, 1983). Thus, diffusion of water vapour in the pore space causes a decrease in d-excess and slight increases in δ18O due to kinetic fractionation (Casado et al., 2021). 3) Sublimation has been widely documented to cause an increase in δ18O of the remaining snow mass due to equilibrium fractionation, and a significant decrease in d-excess due to kinetic fractionation (Ritter et al., 2016; Madsen et al., 2019; Hughes et al., 2021; Wahl et al., 2021; Casado et al., 2021).

An overall increase in δ18O and decrease in d-excess during E10 can be attributed to a combination of 2) and 3) based on observation of net-sublimation and high amplitude diurnal temperature gradient variability indicating vapour transport within the pore space. The period between 9th June at 15:18 UTC and 10th June 10:40 UTC recorded net deposition corresponding to an overall decrease in δ18O during the first day and minimal decrease in d-excess, potentially due deposition of atmospheric water vapour (Stenni et al., 2016; Feher et al., 2021; Casado et al., 2021).

A 30% decrease in d-excess corresponds to negligible change in δ18O during E11. Net-sublimation double that of E10 is measured, but with reduced amplitude in both TGs. Moreover, the largest decrease in d-excess occurs after the first day when the surface-subsurface TG is consistently negative. This indicates that vapour diffusion is controlling the isotopic composition, and the effect of equilibrium fractionation during sublimation from the surface only weakly influences the bulk isotopic composition (Casado et al., 2021).”

L414: In my opinion, simply applying this model at other sites goes a bit too far, because site-specific accumulation seasonality/frequency plays a major role for the near-surface metamorphism. I therefore suggest elaborating on the potential and limitations of the SSA decay model for other sites in greater detail in the discussion section.

We fully acknowledge this point from the reviewer, and instead compare to physical based models from the literature. The observed influence of wind-speed on the SSA decay rate is also discussed, with reference to the limitations of such field-based studies. For example, we are limited by persistent moderate winds potentially perturbed the snow surface, as evidenced by 209 out of the 287 sampling days (2017-2019) having maximum wind-speed above 5 ms-1 based on 10-minute mean values. Although there is a low probability of snowdrift up to 6 ms-1 based on the equation below defined by Li and Pomeroy (1998), we acknowledge the potential and highlight this as a limitation.

New text: *“The SSA decay model described in this study is intended as an investigation into the in-situ behaviour of surface snow SSA through time.”*

L419: While you state earlier that d-excess varies with d18O at the beginning of the season and with SSA later during summer, you state that mainly SSA and d-excess are coupled. Please be consistent with your earlier interpretation here.

We apologise for the inconsistency here. The text has been edited to reflect the different regimes between the sampling years, where for 2019 the SSA and d-excess are coupled, while the *δ18*O and d-excess are coupled during 2018. We propose to remove any generalisation and focus instead on the potential causes for the opposing regimes. We discuss the EOF results in the context of the isotopic change during the SSA decay events to improve the coherence of the discussion.

When it comes to supplementary material, I could imagine a more detailed presentation of the AWS data to be helpful for readers as a meteorological background for this study. Figure A1 is already a good start, which a bit more of a description would help.

The supplementary information has been extended, with a number of plots to support

statements in the paper, specifically the covariance between principal components and wind-speed distributions for 10-minute data and the daily maximum values. In-text references to these figures have been updated and we hope this helps with clarity for explanations.

Technical details

L20: 'first order parameters' - here and in other parts of the manuscript, a hyphen is required ('first-order').

The text has been changed to "first-order parameters".

L105: As you are describing a value range here, an en-dash is needed for 2 -15–130 m kg . Same applies for value ranges throughout the manuscript.

All ranges presented in the manuscript have been corrected for this mistake.

L116: To avoid any misreading, I suggest that the equation is placed in a separate line and to replace the en-dash in 'd-excess' on the left side of the equation with a hyphen. This could also be a good place to give the d18O equation.

The d-excess equation has been moved to a separate line, we have ultimately decided not to include the d18O equation given the primary focus on SSA and d-excess.

L121: Since you are talking about events in time, 'where' should be replaced with 'when'.

This has been changed to:" This study focuses on the events when the SSA measurements decrease rapidly".

L132: Equation 1 requires a multiplication sign.

A multiplication sign has been added to equation 1 and the additional equation 2.

$$SSA(t) = SSA_0 \cdot e^{-\alpha t} \qquad SSA(t) = B - A \cdot ln(t + \Delta t),$$

L180: I think it would be helpful to reference that Table A1 is part of the Appendix. This applies here and for all other references to the Appendix/Supplementary Material. L190: 'snow fall' should be corrected to 'snowfall'.

The accumulation plot has been corrected and incorporated into the description of meteorological conditions at the start of the results. The supplementary material now includes the Table describing event conditions based on field diary observations, the relationships between the principal components from the EOF analysis, and the spatial variance of each relevant parameter (SSA, d18O and d-excess).

Please go through the entire manuscript once more and check:

The proper use and non-use of articles to achieve concise language; Inserting spaces between values and units; Introducing abbreviations when first used, both in the text and in figure captions.

We apologise for errors in the text. The revised manuscript will be thoroughly checked for all the above.

Exploring the role of snow metamorphism on the isotopic composition of the surface snow at EastGRIP

Romilly Harris Stuart[1,4], Anne-Katrine Faber[2], Sonja Wahl[2], Maria Hörhold[3], Sepp Kipfstuhl[3], Kristian Vasskog[4], Melanie Behrens[3], Alexandra Zuhr[5,6], and Hans Christian Steen-Larsen[2]

[1]Laboratoire des Sciences du Climat et de l'Environnement, UMR8212, CNRS – Gif sur Yvette, France
[2]Geophysical Institute, University of Bergen and Bjerknes Centre for Climate Research, Bergen, Norway
[3]Alfred-Wegener-Institut Helmholtz-Zentrum für Polar- und Meeresforschung, Bremerhaven, Germany
[4]Department of Geography, University of Bergen, and Bjerknes Centre for Climate Research, Bergen, Norway
[5]Alfred-Wegener-Institut Helmholtz Zentrum für Polar- und Meeresforschung, Research Unit Potsdam, Telegrafenberg A45, 14473 Potsdam, Germany
[6]University of Potsdam, Institute of Geosciences, Karl-Liebknecht-Str. 24-25, 14476 Potsdam-Golm, Germany

Correspondence: Romilly Harris Stuart (Romilly.Harris-Stuart@lsce.ipsl.fr)

Abstract.

Stable water isotopes from polar ice cores are invaluable high-resolution climate proxy records. Recent studies have aimed to improve knowledge of how the climate signal is stored in the water isotope record by addressing the influence of post-depositional processes on the surface snow isotopic composition. In this study, the relationship between ~~changes in surface snow microstructure after precipitation/deposition events~~ surface snow metamorphism and water isotopes during precipitation-free periods is explored using measurements of snow specific surface area (SSA). Continuous daily SSA measurements from the East Greenland Ice Core Project site (EastGRIP) situated in the accumulation zone of the Greenland Ice Sheet during the summer seasons of 2017, 2018 and 2019 are used to develop an empirical decay model to describe events of rapid decrease in SSA, ~~driven predominantly by vapour diffusion in the pore space and atmospheric vapour exchange.~~ linked to snow metamorphism. The SSA decay ~~model is~~ is best described by the exponential equation ~~$SSA(t) = (SSA_0 - 26.8)e^{-0.54t} + 26.8$. The model performance is optimal for daily mean values of surface temperature in the range 0 °C to -25 °C and wind speed < 6 m s^{-1}. The findings from the SSA analysis are used to explore the influence of surface snow metamorphism on altering the isotopic composition of surface snow. It is found that rapid SSA decay events correspond to decreases in d-excess over a 2-day period in 72 % of the samples. Detailed studies~~ $SSA(t) = (SSA_0 - C)e^{-\alpha t} + C$, and has a dependency on temperature and wind-speed. The relationship between surface snow SSA and snow isotopic composition is primarily explored using Empirical Orthogonal Function (EOF) analysis~~revealed a coherence between the dominant mode of variance of SSA and d-excess during periods of low spatial variability of surface snow over the sampling transect,~~. A coherence between SSA and d-excess is apparent during 2019, characterised by above-average temperatures and increased sublimation rates, suggesting that processes driving change in SSA also influence ~~d-excess.~~ d-excess. Moreover, we observed changes in isotopic composition consistent with fractionation effects associated with sublimation and vapour diffusion during periods of rapid decrease in SSA. Our findings highlight the need for future studies to decouple the processes driving surface snow metamorphism in order to quantify the fractionation effect of individual processes on the snow isotopic composition.

1 Introduction

The traditional interpretation of stable water isotopes in ice cores is based on the linear relationship between local temperature and ~~first order~~ first-order parameters δ^{18}O and δD of surface snow on ice sheets (Dansgaard, 1964). ~~The second order parameter d-excess (d-excess = δD - 8 · δ^{18}O) is a result of kinetic fractionation caused by different molecular diffusivities of oxygen and hydrogen and has traditionally been interpreted in ice core records as reflecting moisture source conditions (Merlivat and Jouzel, 1979). Many factors must be accounted for when reconstructing temperature in ice cores,~~ Accurate reconstruction requires consideration of including precipitation intermittency (Casado et al., 2020; Laepple et al., 2018), past variations in ice-sheet elevation (Vinther et al., 2009), sea ice extent (Faber et al., 2017; Sime et al., 2013), and firn diffusion (Johnsen et al., 2000; Landais et al., 2006; Holme et al., 2018). ~~In addition, recent~~ The second-order parameter deuterium excess (*d*-excess) is defined by the deviation from the near-linear relationship between δ^{18}O and δD due to non-equilibrium (kinetic) fractionation (*d*-excess = δD - 8 · δ^{18}O), and is understood to reflect moisture source conditions (Dansgaard, 1964; Merlivat and Jouzel, 197 , snow crystal formation in clouds (Ciais and Jouzel, 1994; Sodemann et al., 2008), and changes in moisture source (Masson-Delmotte et al . Here we focus on processes influencing isotopic composition of the surface snow while exposed to surface processes.

Recent studies have documented isotopic composition change in the surface snow during precipitation-free periods (Steen-Larsen et al., 2014; Ritter et al., 2016; Casado et al., 2018; Hughes et al., 2021), linked to synoptic variations in atmospheric water vapour composition and subsequent ~~snow-vapour exchange (Steen-Larsen et al., 2014). Current research aims to quantify the influence of post-depositional processes on isotopic change of the surface snow (Steen-Larsen et al., 2014; Ritter et al., 2016; Madsen et~~ exchange with the surface snow (Steen-Larsen et al., 2014; Ritter et al., 2016; Madsen et al., 2019; Hughes et al., 2021; Wahl et al., 2021; . Post-depositional processes at the surface involve additional kinetic effects adding complexity to the interpretation of *d*-excess (Hughes et al., 2021; Casado et al., 2021).

~~Surface snow undergoes structural changes , as grains form bonds, grow. This process is called~~ After deposition, snow grains undergo structural changes known as snow metamorphism, which is active at the surface and at greater depths, depending on temperature (gradient) conditions (Colbeck, 1983; Pinzer and Schneebeli, 2009b). ~~A major change the snow is undergoing, is the reduction of the ice-air interface to reduce energy (Legagneux and Domine, 2005)~~We here explicitly refer to snow that is lying at the surface for an unknown amount of time and thus does not directly represent freshly precipitated snow. Surface snow metamorphism initially drives a reduction in the snow-air interface to reach thermodynamic stability (Colbeck, 1980; Legagneux and Domine, 2005). The snow-air interface can be described by the widely used parameter ~~SSA. It is assumed to be linked to the optical grain size equivalent (Linow et al., 2012) and can be utilized~~ snow specific surface area (SSA), which is dependent on optical grain radius and density of ice ($SSA = 6/\rho_{ice} * d_{opt}$) (Gallet et al., 2009), and can be used as a measure for snow metamorphism (Cabanes et al., 2002, 2003; Legagneux et al., 2002). ~~In this study we use SSA to describe the (rapid) change of surface snow as one measure for snow metamorphism.~~

~~This manuscript focuses on surface snow property changes after precipitation. We here explicitly refer to snow which is lying at the surface for an unknown amount of time and thus does not directly represent freshly precipitated snow. Fresh snow crystals have a high value of SSA . After deposition of the crystals on the surface, the SSA rapidly decreases from its~~

initial value due to crystal growth (Cabanes et al., 2002; Legagneux et al., 2004; Domine et al., 2007).The reasons for the SSA decrease are wind-driven fragmentation (Comola et al., 2017; Neumann et al., 2009), interstitial Freshly deposited snow has a high SSA which decreases with time under both isothermal (<10 °C m^{-1}) and temperature gradient (>10 °C m^{-1}) conditions (Cabanes et al., 2002; Legagneux et al., 2004; Domine et al., 2007; Genthon et al., 2017). Decrease in SSA is predominantly the result of Ostwald Ripening, where large grains grow at the cost of smaller grains (Lifshitz and Slyozov,1961; Legegneux et al., 2004), vapour diffusion in the pore space between snow crystals (Pinzer et al., 2012; Flin and Brzoska, 2008) and sublimation (Sokratov and Golubev, 2009). driven by sublimation and deposition (Flin and Brzoska, 2008; Sokratov and Golubev, 2009; Pinzer et al., 2 , and wind effects (Picard et al., 2019). Under natural conditions, SSA decrease is driven by a combination of these processes depending on surface conditions (Cabanes et al., 2003; Pinzer and Schneebeli, 2009a), each potentially modifying the isotopic composition of the snow (Ebner et al., 2017).

Models can provide a quantitative description of the rapid SSA decrease after precipitationdeposition. Previous studies have proposed SSA decay models using a combination of field measurements and controlled laboratory experiments (Cabanes et al., 2002, 2003; Legagneux et al., 2003, 2004; Flanner and Zender, 2006; Taillandier et al., 2007). While current versions of the so-called decay models exist, these are mostly based on lab-experiments and non-polar snow observations. Exponential models to describe SSA decay are documented to be the best fitting to in-situ data (Cabanes et al., 2003). However, the lack of a physical basis led Legagneux et al. (2003) to construct a theoretical equation to describe SSA decay based on grain growth theory, which was then developed by Flanner and Zender (2006) who defined parameters based on surface temperature, temperature gradient and snow density.

Existing SSA decay models have not yet been extensively applied to polar ice sheet surface snow. Conditions for surface snow on polar ice sheets such as Greenland are however are not necessarily comparable to other alpine regions. The dry-accumulation zone of the Greenland ice sheet has only small amounts of intermittent precipitation. Furthermore, the and Arctic regions regarding negligible melt and the high-latitude radiation budgetis different than in other alpine regions.

Only few continuous datasets of daily . Moreover, while continuous surface SSA measurements exist from the remote regions of the polar ice sheets (Libois et al., 2014; Picard et al., 2014). While SSA observations from Greenland exist (Carmagnola et al., 2013; Lin , diurnal datasets covering multiple months and years provide a better foundation for Antarctica (Gallet et al., 2011, 2014; Picard et al., 2014 , those from Greenland focus on the depth evolution of SSA (Carmagnola et al., 2013; Linow et al., 2012). Continuous datasets of daily SSA and corresponding isotopic composition measurements from the accumulation zone of the Greenland Ice Sheet can contribute to understanding the relevance of snow metamorphism for ice core studies. In particular, studies of SSA and snow metamorphism from Greenland are relevant for isotope surface energy budget and for ice core studies. This is because snow metamorphism is expected to influence the snow isotopic composition as The latter is of particular interest owing to observations of isotopic fractionation during snow metamorphism documented in laboratory studies (Ebner et al., 2017) and field experiments (Hughes et al., 2021). Nonetheless, few studies have focused on the direct relationship between physical snow properties, such as SSA, and post-depositional changes in isotopic composition.

An SSA decay model optimized for Greenland conditions would provide a better quantitative foundation for a process-based understanding of surface snow metamorphism on Greenland. Furthermore, a quantitative description of Greenland SSA decay

would provide a basis to explore how snow metamorphism at the surface plays a role for the alteration of isotopic composition of Greenland snow after deposition.

In this manuscript, the aim is to explore the behaviour of surface snow metamorphism on polar ice sheets using daily SSA measurements , and compare from Northeast Greenland during summer and compare the change in physical properties to the isotopic composition measurements. The primary focus is to document events where changes in SSA occur rapidly over a duration of a few over a number of days. We first identify events of rapid SSA decreases (decays) and explore how the isotopic composition of the snow changes during these events. Periods of rapid decrease in SSA are used as a proxy for snow metamorphism. Using daily field observations of snow properties from Northeast Greenland during summer, events of Events of rapid SSA decrease (SSA decay events) are used to 1) quantify and model surface snow metamorphism in polar snow and, 2) assess isotopic change during surface snow metamorphism. The data presented here has the potential to contribute to the understanding of the influence of post-depositional processes on physical and isotopic changes in the polar ice sheet surface snow. This allows for better understanding of snow properties at remote regions of polar ice sheets , and contributes and contributes to the interpretation of water isotopes in polar ice cores.

2 Study site and methods

2.1 EastGRIP site overview and meteorological data

All data used in this paper were collected as part of the Surface Program corresponding to the international deep ice core drilling project at the East Greenland Ice Core Project site (EastGRIP 75.65°N, 35.99°W; 2,700 m.a.s.l) during summer field seasons (May-AugustMay-August) of 2017, 2018 and 2019. The accumulation rate is approximately 14 cm w.eq. yr^{-1} (Schaller et al., 2017).

Meteorological data used for this study are from the Program for Monitoring of the Greenland Ice Sheet (PROMICE) Automatic Weather Station set up by the Geological Survey of Denmark and Greenland (GEUS) at EastGRIP in 2016 (Fausto et al., 2021). The data are 10-minute mean values for a multitude of variables. Snow temperature was measured using a thermistor string at 0.1 m intervals during 2017 and 2018 but was modified to 1 m intervals in 2019. An additional thermistor string was thus installed in May of 2019, from which we use the 0.1 m measurements. Instrument specifics can be found in Fausto et al. (2021). Mean weather conditions vary between sampling years, as outlined in Table 1. Instrument specifics can be found in Fausto et al. (2021). Mean summer surface temperatures for 2019 were -10.6±5 °C, 5 °C higher than 2017 and 2018. Westerly winds prevail , with mean wind speed of 4.5 m s^{-1} (Madsen et al., 2019). during 2017 and 2018 with a wind direction of 227 °N, while 2019 had a prevailing south-westerly wind (239 °N), corresponding to opposing phases of the North Atlantic Oscillation (NAO).

An Eddy-Covariance tower eddy-covariance (EC) measurement tower was set up at EastGRIP in 2016. The relevant variable measured from this system is 2016 to measure wind and humidity fluxes (Madsen et al., 2019; Wahl et al., 2021). Here we use the 30–minute latent heat flux (LHF) which is directly determined by LE) measurements which are calculated from the measurement of humidity fluxes between the surface and atmosphere. Positive LHF LE indicates upwards energy flux in the

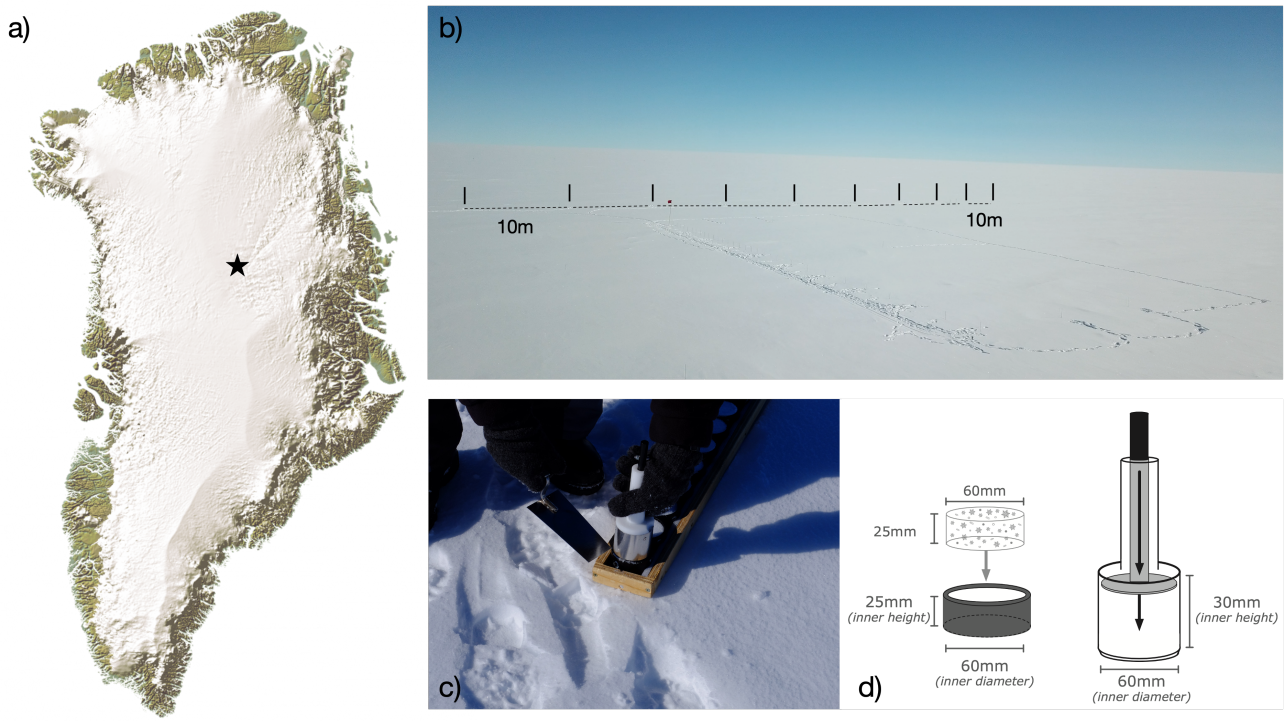

Figure 1. *SSA Sampling Procedure*

a) A map of Greenland with a black star indicating the EastGRIP site (Source: ~~Eric Gaba – Wikimedia Commons user: Sting~~VisitGreenland). b) A photograph of the clean snow area at the field site (Credit: Bruce Vaughn), with black lines indicating the SSA sampling transect with 10 m spacing shown as dashed lines. c) A photograph of SSA sampling cups (Credit: Sonja Wahl), and d) an illustration of the sampling device from Klein (2014).

form of sublimation in Table 1. ~~All field seasons had net sublimation, with the highest magnitude observed in 2019 (See Data Availability Section A).~~

Significant weather conditions such as ground fog, drifting snow and snowfall, were documented each day in the EastGRIP field diary.

2.2 Snow sampling procedure

Each summer season of 2017, 2018 and 2019 snow samples were taken once a day from May to August at 10 sampling sites, each marked by a stick, along a 90 m transect with 10 m spacing upwind of the EastGRIP camp to ensure clean snow (Fig. 1b). The specific dates for each season are given in Table 1. The precise location of each sample was marked by a small stick to ensure the adjacent snow is sampled the next day and to avoid sampling snow from different depths. A 6 cm diameter sampling device collected the top 2.5 cm of surface snow (Fig. 1c). Snow density is determined using the weight of each snow

Table 1. *Weather statistics - 2017, 2018 and 2019* ~~The table present the mean and standard deviation for the weather variables, surface temperature, humidity with respect to ice, wind speed and latent heat flux. Surface temperature and wind speed are from the PROMICE weather station based on measurements during the field seasons of 2017, 2018 and 2019. Relative humidity with respect to ice is calculated from vapour pressure of the air and sa vapour pressure over ice. Latent heat flux is taken from the EC tower dataset.~~

		2017	2018	2019
	Instrument	*06/05 - 05/08*	*04/05 - 07/08*	*24/05 - 01*
~~*Mean Mean Mean*~~ height**Surface Temperature** (°C)	(Kipp and Zonen CNR1/CNR4 radiometer)	-14.5 ± 6.2	-15.76 ± 7.6	-10.6 ± 5
Relative Humidity (~~with respect to ice) (%~~%)	(Calculated)	~~96~~ 95.8 ± 15	~~96~~ 95.9 ± 16	~~94~~ 93.3 ±
Wind Speed ($\mathrm{m\,s^{-1}}$)	(R.M. Young 05103-5 ±0.3 $\mathrm{m\,s^{-1}}$)	4.9 ± ~~. 2~~ 0.2	4.2 ± 1.9	4.5 ± 1.6
Latent Heat Flux (~~$W\,m^{-2}$~~ $\mathrm{W\,m^{-2}}$)	~~1.3~~ (IRGASON Campbell Scientific)	1.28 ± ~~4~~ 4.2	~~1.1~~ 1.3 ± ~~3.9~~ 4.3	2.6 ± ~~5.9~~ 5

Mean and standard deviation for weather variables, surface temperature (calculated from upwards and downwards long-wave radiation with long-wave em set to 0.97), relative humidity, wind speed and latent heat flux during the three sampling seasons. Surface temperature, relative humidity and wind sp PROMICE weather station based on 10-minute measurements. Latent heat flux an upwards flux from the eddy-covariance tower.

sample with a known volume. At the start of each season, sticks were placed at each site and snow height was determined by the distance between the snow surface and top of the stick. Accumulation was calculated using the cumulative sum of the daily difference between measurements of snow height from each site. The resultant datasets consist of 10 daily measurements of three parameters, SSA, density and accumulation, over a ~~92, 100~~ 89-, 94- and 66-day period for 2017, 2018 and 2019 respectively.

~~Although samples were measured each day, the exact sampling timevaries. Snow sampled during the afternoon would have had extended time exposed to solar radiation maximum, compared to snow sampled during~~ The samples were all taken in the day time, primarily in the morning. ~~Furthermore, the sampling time has implications for capturing precipitation events.~~ The meteorological data is re-sampled to the SSA sampling time-periods to ensure consistent comparison.

2.3 SSA measurements

2.4 ~~Ice Cube calibration~~

Each snow sample is placed into the Ice Cube sampling container below an Infra-Red (IR) laser diode (1310 nm), where the SSA is calculated based on IR hemispherical reflectance, explained in Gallet et al. (2009), while information on the Ice Cube device can be found in Zuanon (2013). ~~Light penetration depth~~ The *e*-folding depth of 1310 nm radiation in snow of 200 $\mathrm{kg\,m^{-3}}$ is approximately 1 cm ~~(Gallet et al., 2011), resulting in a measurement of the top <1 cm of each sample (Mean snow density at EastGRIP~~ (Gallet et al., 2009). The mean snow density from 2017, 2018 and 2019 ~~=~~ is 293 $\mathrm{kg\,m^{-3}}$ (307 ± 40 $\mathrm{kg\,m^{-3}}$, 278 ± 47 $\mathrm{kg\,m^{-3}}$, 294 ± 50 $\mathrm{kg\,m^{-3}}$ ~~)~~for 2017, 2018 and 2019 respectively), resulting in each measurement being heavily weighted to the top <1 cm of the 2.5 cm sample. The light reflected from the snow samples is converted into inter-hemispheric IR reflectance using a calibration curve based on methane absorption methods (Gallet et al., 2009). A radiative-transfer model is used to

retrieve SSA from inter-hemispherical IR reflectance. To avoid influence from solar radiation, SSA was measured inside a ventilated white tent kept at temperatures between -5 °C and -10 °C. SSA measurements have an uncertainty of 10 % for values between ~~5-130~~5–130 $m^2\,kg^{-1}$ (Gallet et al., 2009).

2.4 Surface snow isotopes

~~Samples collected following the sampling procedure outlined in Section 2.2 were also used for isotopic composition measurements, resulting in~~ Individual SSA samples were put in separate bags and subsequently sampled for water isotopic composition. Thus, every day the 10 ~~daily isotope measurements taking~~ SSA samples have a corresponding isotopic composition. The resultant isotope value is the average composition over the top ~~25~~2.5 ~~mm~~ cm of snow. Each sample was sealed in polyethylene bags to avoid any air to equilibrate with the snow and affect the isotopic composition. All samples were kept frozen during transportation and storage.

After melting, each bag was shaken to ensure the isotopic composition of the sample is representative. 1.25 μl of each sample was then pipetted into a vial ready for isotopic analysis. The snow samples were then analysed at Alfed Wegener Institute in Bremerhaven using a cavity ring-down spectroscopy instrument model Picarro L-2120-i and L-2140-i following the protocol of Van Geldern and Barth (2012). This technique is used to obtain measurements of δ^{18}O and δD with an uncertainty of 0.15‰ and 0.8‰ respectively. ~~d-excess is calculated by the equation $d-excess = \delta D - 8 \cdot \delta^{18}$O with a resultant~~ The calcualted values for *d*-excess have an uncertainty of 1‰. Observing relationships between our SSA and isotope data requires consideration for the depth offset between the SSA measurements and the isotopic composition measurement which measures the entire 2.5 cm snow layer.

2.5 Data analysis

2.6 ~~Data analyses~~

2.5.1 Defining SSA decay events

~~This study focuses on the events where the SSA measurements decay rapidly over a duration of a few days. SSA decays are here defined as the events where the 2-day change of daily mean values are higher than a given threshold. This threshold is the same value for all years and is calculated based on the~~ To systematically identify rapid decreases in SSA, which we use as a proxy for events of snow metamorphism after deposition (identified based on the high mean SSA values), a threshold is set using the bottom 10th ~~percentile of the decays and set at~~ percentile of SSA decreases over a two-day period (-13 $m^2\,kg^{-1}$ ~~2-day^{-1}. If the daily mean changes over a 2-day period is higher than the threshold, then this period is selected as a rapid SSA decay event. The duration of the event is set to start at the rapid decay and end on~~ 2-day^{-1}). This was found to result in the most equal number of events from each sampling year compared to 1- and 3-day changes. SSA decay events are defined as by the initial peak, identified by the threshold, through to the next increase in SSA (rather than decrease).

We here use the term deposition events to describe rapid increases in SSA, expected to be from precipitation, drifted snow or hoar formation. Previous studies have indicated that surface hoar and sublimation crystal-like grain growth features at the surface have an SSA value around $54\,m^2\,kg^{-1}$, based on the ~~day when the mean SSA measurements increase (rather than decrease) again.~~ SSA of hoar frost (Domine et al., 2009). Accumulation data and field observations are used to identify the initial conditions.

A set of criteria are required to reduce the potential of analysing events with wind-perturbed surfaces, resulting in the removal of surface snow. In Antarctica, unconsolidated surface snow has been observed to drift at wind speeds as low as $5\,m\,s^{-1}$ measured at 2 m height (Birnbaum et al., 2010). However, a study from Greenland documented snowdrift starting at $6\,m\,s^{-1}$ (Christiansen, 2001), likely due to warmer temperatures allowing for the surface snow to become more bonded (Li and Pomeroy, 1997). At EastGRIP, calm conditions correspond to wind speeds from 0–$5.2\,m\,s^{-1}$ according to field diary observations. The mean daily maximum wind speed for the three sampling seasons was $6.8\,m\,s^{-1}$, while blowing snow was documented only when wind speeds exceeded $7\,m\,s^{-1}$.

Based on this assessment, we define two wind-speed categories for comparison of the effects of wind-speed on SSA decrease. The first includes events with wind-speed consistently below $5.2\,m\,s^{-1}$, hereafter referred to as low-wind events, to ensure no surface perturbation. Secondly, we consider events where the maximum wind-speed is between 6–$7\,m\,s^{-1}$, hereafter referred to as the moderate-wind events. The inclusion moderate-wind events allows an assessment of the influence of wind-speed on SSA decrease.

2.5.2 Modelling surface snow metamorphism

The first empirical SSA decay model was proposed by (Cabanes et al., 2003) who described a temperature-dependent exponential decay based on snow samples collected from the Alps (Cabanes et al., 2002) and Arctic Canada (Cabanes et al., 2003). A following logarithmic equation (Eq. (2)) fit controlled to laboratory experiments was proposed by (Legagneux et al., 2003), where parameters A and B were found to be arbitrarily related to the decay rate and initial SSA of each sample, and are linearly correlated at -15 °C.

$$SSA(t) = SSA_0 \cdot e^{-\alpha t} \tag{1}$$

$$SSA(t) = B - A \cdot ln(t + \Delta t) \tag{2}$$

To improve the physical basis of the model, the theory of Ostwald Ripening, describing grain growth driven by a physical need to reduce surface energy, was implemented into the model (Legagneux et al., 2004). The equation (Eq. (3)) has two parameters τ and n; τ is the decay rate and n relates to theoretical grain growth. The physical model was developed by Flanner and Zender (2006) to incorporate more specific physical quantification to the parameters to include information about

temperature, temperature gradient, and density. Based on these three conditions, they created a look-up table for τ and n.

$$SSA(t) = SSA_0 \left(\frac{\tau}{t+\tau} \right)^{1/n} \quad (3)$$

Taillandier et al. (2007) proposed two equations based on the logarithmic model, defined by Legagneux et al. (2004), to define the decay rate under isothermal and temperature gradient conditions where they were able to directly incorporate a surface temperature parameter.

An empirical decay model is constructed building upon previous studies (Cabanes et al., 2002, 2003; Flanner and Zender, 2006; Legagneux et al., 2002, 2003; Taillandier et al., 2007). This model uses continuous daily SSA measurements from EastGRIP to describe the behaviour of surface snow SSA in polar summer conditions. ~~The post-precipitation decreases in SSA are hereafter referred to as decays~~All samples of defined SSA decay events are used to quantify surface snow metamorphism.

$$SSA(t) = SSA_0\, e^{-\alpha t}$$

3 Results

~~Eq. (1) is proposed by Cabanes et al. (2003) as the most accurate description of SSA decay, where SSA_0 is the initial SSA value, α the decay rate. To best describe grain coarsening and the processes of sublimation and deposition driving mass redistribution of a new snow layer, days with mean wind speeds above 6~~

3.1 EastGRIP conditions

Meteorological variables over the three sampling seasons vary substantially. Figure 2 shows the 10-minute mean values of air temperature, wind-speed, relative humidity and latent heat flux (LE). The accumulation in Fig. 2d are daily mean values (see Section 2.2). Air temperatures were below 30 °C between May 5th and May 8th, such low temperatures were not recorded for 2017 and 2019. However, when comparing the period from May 27th (start of 2019 season) to August 5th of each year, 2018 air temperatures (-13.3 °C) were still 0.5 °C lower than 2017 and 3.2 °C lower than 2019. Two days during 2019 recorded air temperature above 0 °C.

The 2017 season was characterised by high wind intrusions of $>13\,\mathrm{m\,s^{-1}}$ ~~are removed to reduce the influence of wind redistribution. Individual sample analysis is preferentially used to avoid daily mean values possibly attenuating any signals due to spatial variability in surface snow age. Aged snow patches are expected to respond differently to surface processes than new snow patches due to different original crystal structures at the start of events.~~ at approximately 20-day intervals. Considering all three sampling years, 2017, 2018 and 2019, the average daily maximum wind speed is $7\,\mathrm{m\,s^{-1}}$, with 209 out of the total 237 sampling days having maximum wind speed above $5\,\mathrm{m\,s^{-1}}$. The distributions of daily maximum wind-speed compared to 10-minute mean values are found in the Supplemental Fig. A1. Relative humidity is consistent throughout the years with mean values around 95% and similar variability of $\sim$7%.

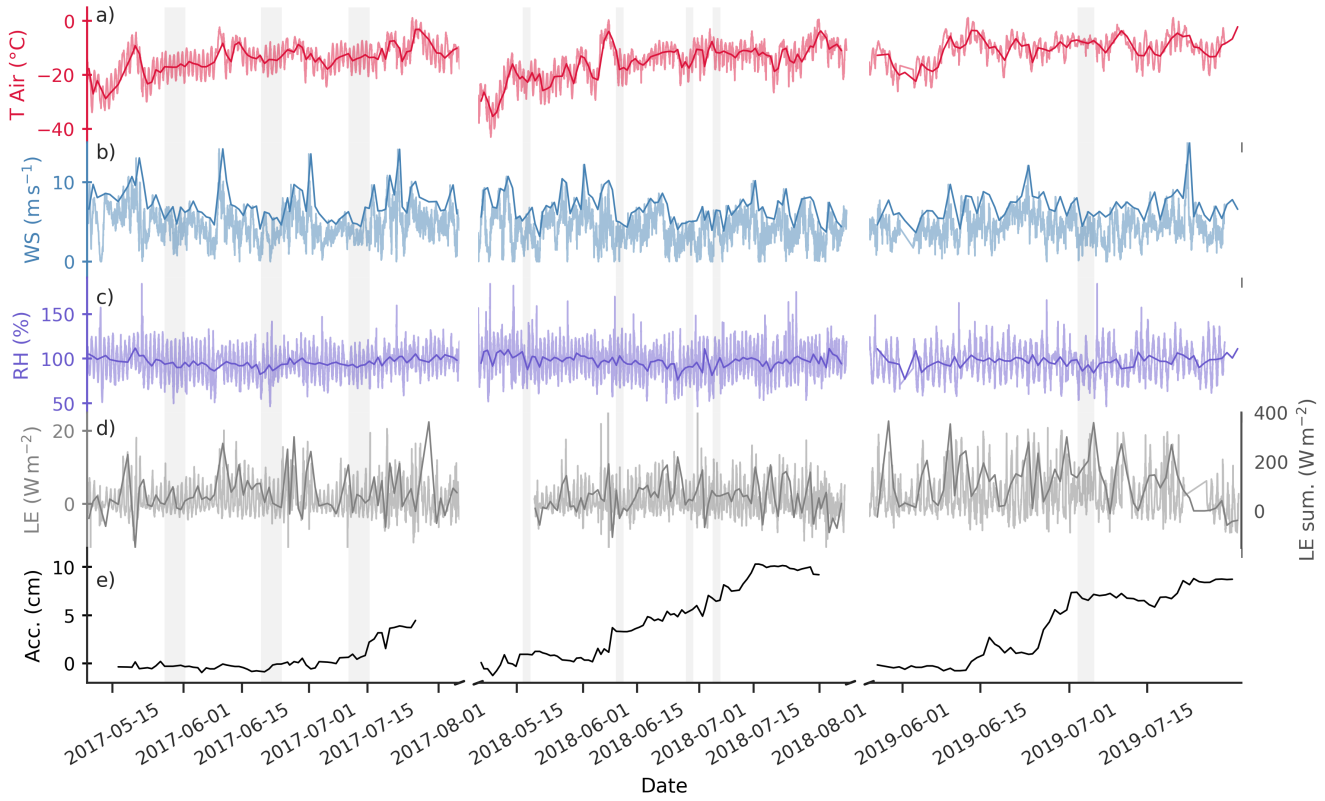

Figure 2. *Meteorological data from 2017, 2018 and 2019*
Data is presented for the specific sampling periods for each year. The 10-minute mean data from PROMICE is shown for air temperature (a), wind-speed (b) and relative humidity (c). The bold lines indicate the mean values, based on the snow sampling time interval, for air temperature and relative humidity, and the maximum value for wind-speed. The Relative humidity is determined from vapour pressure and saturation vapour pressure. Latent heat flux (d) is 10-minute averages from the eddy-covariance tower, with the bold grey line showing the daily sum. Accumulation is presented in panel d).

4 ~~Results~~

3.1 ~~SSA decay events~~

There was a total of 5 cm accumulated snow over the 89-day season of 2017, half the amount of 2018 and 2019. The field season for 2018 started on the 5th of May, 9-days earlier than 2017 (14th May), and 22 days earlier than 2019 (27th May). Substantially more sublimation was recorded in 2019, where the daily sum was approximately double that of 2018.

3.0.1 Spatial and temporal surface variability

SSA data collected at EastGRIP indicate continuous changes in the physical structure of the snow crystals during all sampling seasons, with both temporal and spatial variability. The temporal SSA variability shows changes in physical snow structure with peak values closely associated with precipitation and decreases A recent study at EastGRIP has shown the significant in-homogeneity in surface snow due to post-depositional re-working reworking of the snow . Summer seasonal SSA evolution is presented in Fig. **??** for 2017, 2018 and 2019 with each faded line representing individual samples (10 per day), and the bold line showing the daily mean. Spatial variability between sites is most prevalent when there are high SSA values, indicating fresh snow.

A total of 21 rapid SSAdecay events are identified, with 6(Zuhr et al., 2021). To avoid attenuation of isotopic signal, each sample is treated independently. Using a confidence interval of 95% ($p<0.05$), the relationship between SSA and isotopic

Figure 3. *SSA Timeseries 2017, 2018 and 2019*Time-series of SSA time-series between May and August for (a)2017, d18O (b)2018 and , *d*-excess (c) 2019. Faded lines represent and the 10 individual samples from principal components (PC1) of each variable (d). For each plot, the 90 m markers indicate the individual sampling transect, while sites and the bold line link shows the daily meanvalues. Gaps The secondary y-axis in panel a) shows the timeseries represent missing dataaccumulation. Grey The grey bars highlight indicate the periods of decrease in SSA defined by the threshold algorithm for each year. Six decrease decay eventsare observed in 2017 and 2019, while nine are observed in 2018. Decrease events are interpreted as rapid grain growth due to snow metamorphism, and stars indicating days with precipitation.

composition is tested using Empirical Orthogonal Function (EOF) analysis. The purpose of EOF analysis is to identify the dominant modes of variance in both the temporal and spatial dimensions for each parameter - SSA, ~~9 and 6 events for~~ $\delta^{18}O$ and d-excess - which are all measured from the same sample.

All parameters continuously change throughout the field seasons of 2017, 2018 and 2019 ~~respectively.Grey bars in Fig. ?? highlight events defined by the decrease threshold.~~ (Fig.3), with large spatial variability in isotopic composition. SSA is characterised by peaks, often corresponding to large spatial variability, followed by gradual decreases over a number of days, a feature which is most prominent during 2017 and corresponds to negligible accumulation. The amplitude of SSA variability is largest in 2019. The start of the 2018 season has very high SSA values (daily mean $88\,m^2\,kg^{-1}$) corresponding to low and homogeneous $\delta^{18}O$. Maximum SSA values ~~for~~ of individual samples for 2017, 2018 and 2019 are ~~92~~$85.3\,m^2\,kg^{-1}$ ~~and 82, $95.3\,m^2\,kg^{-1}$ respectively, while during 2017 there are only two instances of daily mean SSA being above 60^{-1}~~ and $86.7\,m^2\,kg^{-1}$ respectively.

~~A visual inspection of the decay events~~ Inter-annual variability is observed in $\delta^{18}O$, with seasonal mean values of -31.6‰, -32.7‰ and -27.3‰ for 2017, 2018 and 2019 respectively (Fig. 3a). Note that the 2019 field season started approximately 15 days later than 2017 and 2018, resulting in a bias towards mid-summer conditions. Throughout the season $\delta^{18}O$ follows a gradual increasing trend from May to August. Some cases of abrupt decreases (-10‰) are observed in the late summer, for example, on July 12th in 2018 and July 25th in 2019. No clear seasonal trend is observed in d-excess (Fig. 3b) but with periods of gradual decreases. Total daily spread in $\delta^{18}O$ and d-excess is approximately 15‰.

The spatial and temporal principal components of each variable are presented in Fig. ~~?? indicates a relationship between initial SSA and subsequent magnitude of decrease. To test whether the mechanisms of decay are consistent throughout events, observed SSA decays are analysed to construct an empirical model.~~ 3d. During 2017, 2018 and 2019 all variables have one dominant mode of variance, or principle component (PC1). PC1 of SSA ($PC1_{SSA}$) explains 61 %, 77 % and 72 % of variance for the respective years, PC1 of $\delta^{18}O$ ($PC1_{\delta^{18}O}$) explains 69 %, 83 % and 75 % of the total variance respectively, while PC1 of d-excess ($PC1_{d-excess}$) explains 47 %, 51 % and 60 %.

Distinct differences are observed between the sampling years, most prevalent is the opposing regime from 2018 to 2019. During 2018 $PC1_{\delta^{18}O}$ and $PC1_{d-excess}$ exhibit a significant relationship, with a strong negative correlation for the spatial component of $PC1_{\delta^{18}O}$ and $PC1_{d-excess}$. A significant relationship is also observed for the temporal component of $PC1_{SSA}$ and $PC1_{\delta^{18}O}$. In contrast, data from 2019 are characterised by significant relationships between $PC1_{SSA}$ and of $PC1_{d-excess}$ in both the spatial ($r=0.75$) and temporal dimensions. No relationship is observed between $PC1_{\delta^{18}O}$ and $PC1_{d-excess}$ during 2019. For 2017, significant relationships ($p<0.05$, 95% confidence) are observed between the temporal component of $PC1_{SSA}$ and $PC1_{d-excess}$, and the temporal and spatial component of $PC1_{\delta^{18}O}$ and $PC1_{d-excess}$. A shift is observed after July 15th where $PC1_{d-excess}$ changes from co-varying with $PC1_{\delta^{18}O}$ to $PC1_{SSA}$.

3.1 SSA decay events

3.2 ~~EastGRIP SSA decay model~~

Continuous SSA measurements allow for the construction of an empirical model to describe SSA decay at EastGRIP through time while exposed to surface processes. ~~All samples of defined SSA decrease events defined in Section 3.1 are used to quantify surface snowmetamorphism. For all events with mean temperature above -25~~A visual inspection of the SSA decay events highlighted in Fig. 3a indicates a relationship between initial SSA and subsequent magnitude of decrease. Prior to analysis, we assess the meteorological conditions and field observations to remove SSA decay events with potentially perturbed surface snow. This includes all events coinciding with observations of ground fog, snowdrift, and snowfall (indicated in Fig. 3), and events where the wind-speed exceeds the thresholds defined in Section 2.5.1.

From the years 2017, 2018 and 2019 a total of 21 events are identified that fulfil the SSA decay criteria (as defined in Section 2.5.1). These events are named E1, E2 etc (see Table A for more information on the individual events). Exploring weather conditions for these events reveals that 12 out of the 21 events are influenced by either snowdrift, snowfall, or ground fog according to field diary observations. Of the remaining 9 events, two are in the low-wind category (E10 and E11 ~~°C, the mean SSA of the final day is around 30~~=5.1 $\mathrm{m\,s^{-1}}$), and 7 in the moderate-wind category. Both E10 and E11 had consistent clear sky conditions. We note here that E11 was preceded by significant ground fog, not snowfall, indicating that the peak value of 46 $\mathrm{m^2\,kg^{-1}}$ ~~(referred to as the background decay state). A relationship is observed between the~~ was likely the result of surface hoar, and thus, rapid SSA decay follows an SSA peak not caused by precipitation.

SSA samples are treated individually to quantify SSA decay rate for the different categories. The rate of SSA decay is closely linked to the SSA value at the start of each event (initial SSA vs. magnitude of decrease during the decay period ~~$r^2 = 0.4$)~~ (Fig. 4), suggesting the rate of change is proportional to the absolute value, as described by exponential decay law (r=-0.71 and r=-0.84 for low- and moderate-wind events respectively) (Cabanes et al., 2003).

The mean air temperature for all SSA decay events was between -20.8 °C and -7 °C. The first day of each event is characterised by the largest change in SSA, followed by a decrease in magnitude over the subsequent days. This feature is most apparent for the longer events (E1, E2 and E4), where SSA has minimal change below 25 $\mathrm{m^2\,kg^{-1}}$.

~~SSA decay~~

3.2 EastGRIP SSA decay model

SSA decay rate is quantified by plotting the rate of change in SSA per day against the absolute SSA value for all 10 sampling sites for ~~all~~ low- and moderate- wind events (Fig. 4a). We observe a linear relationship between the rate of change in SSA per day (ΔSSA) and SSA. ~~Outliers are measurements from days with mean air temperature below -25 °C as highlighted in Fig. 4a. This observation is in agreement with theoretical understanding of snow crystal formation transitioning from dendrites to columns at approximately -22 °C (Domine et al., 2008). We therefore define the SSA decay model for a temperature range between -25 °C and 0 °C and daily mean wind speeds below 6 $\mathrm{m\,s^{-1}}$ based on hourly averaged values.~~ An overview of event conditions using field observations are presented in Table A.

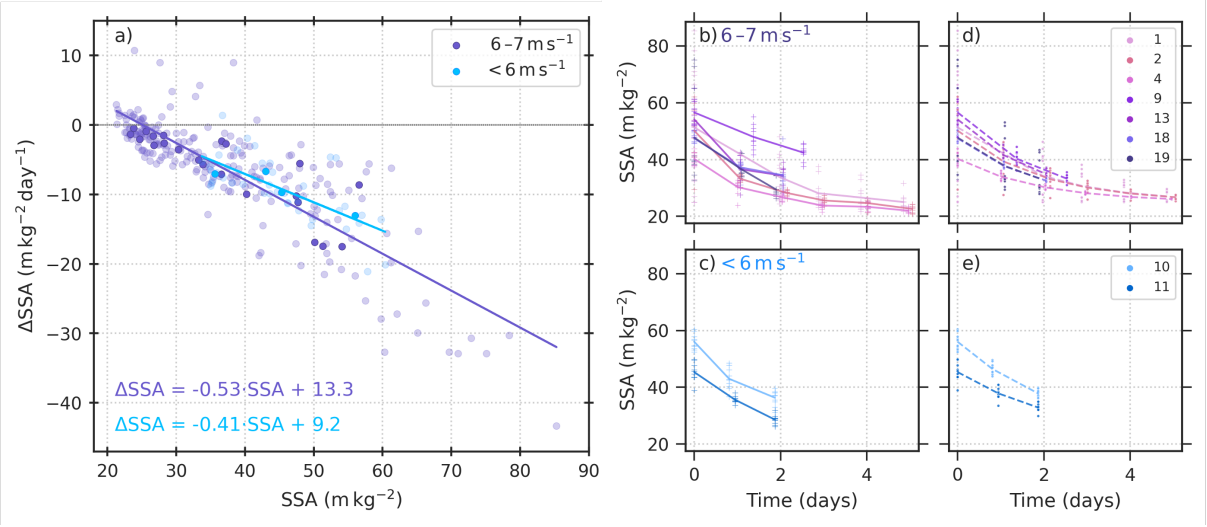

Figure 4. *Decay Model Construction and Predictions*
Linear regressions for change in SSA against the SSA for the low-wind (blue) and moderate-wind (purple) SSA decay events (a). Filled markers indicate the daily mean values and transparent markers show the individual samples sites. The observed SSA decays are show for the moderate-wind events (b), and the low wind events (c), followed by the modelled SSA decays for the respective events in d) and c). The legend in d) and e) indicates the SSA decay event number, presented in Table A

~~Constructing the~~ The SSA decay model for EastGRIP is ~~based on~~ constructed using the differential equation for the linear relationship between ΔSSA and absolute SSA~~which is defined as Eq. (??).~~. Solving the differential with respect to time (t), produces the SSA decay model defined as Eq. (4), which follows the equation structure ~~from~~ of Eq. (1).

$$\frac{dSSA}{dt} SSA(t) = -0.54\,(SSA_0 - C)\,e^{-\alpha \cdot t} + 14.69\,C \tag{4}$$

$$SSA(t) = (SSA_0 - 26.8)\,e^{-0.54t} + 26.8$$

Where SSA(t) is the SSA measurement at a given time, SSA_0 is the initial SSA value, ~~and -0.54~~α is the decay rate, and C is the constant. The decay rate, determined by the slope of the linear regressions in Fig. 4, is higher for moderate-wind SSA decay events (-0.53 $m^2\,kg^{-1}\,day^{-1}$~~is the decay rate (α), as defined by the slope of Eq. (??).~~) than for low-wind SSA decay events (-0.41 $m^2\,kg^{-1}\,day^{-1}$). To account for a non-zero decay constant, ~~the value 26.8 $m^2\,kg^{-1}$~~ C describes the 'background' SSA state which is defined by the value of x when the linear regression crosses the ~~y-axis~~ (y-axis in Fig. 4a~~). The SSA decay model describes rapid decrease in SSA based on empirical data from EastGRIP, Greenland.~~

3.2.1 ~~Model evaluation~~

~~*Decay Model Construction and Predictions*All samples for all events are included in plot a) showing the relationship between the rate of change in SSA per day (ΔSSA day^{-1}) against the daily absolute values. Points are coloured by the daily mean surface temperature. The linear regression is based on values for surface temperatures between -25 °C and 0 °C, and daily mean wind speeds below 6 m s^{-1}. b) shows a comparison between the model predicted SSA values using Eq. (4), against the SSA observations. The marker colour represents the day of the events (DOE). Marker style represents the sampling year to assess inter-annual variability for 2017 (o), 2018 (x) and 2019 (□). c), d) and e) show all included events in full-line and f), g) and h) show the model predictions as the dashed line. E1-E21 refers to events as listed in Table A. Missing data day-1 E1.~~

~~Model performance is tested by comparing daily predicted decrease to the 10 daily observations. Model-data residuals for daily data are normally distributed, suggesting no systematic errors in model predictions. Figure 4 shows the construction of the model (Fig.4,a-b) and prediction of SSA decay (Fig. 4,f-h).~~ , equal to 21 m^2 kg^{-1} and 24 m^2 kg^{-1} for low- and moderate-wind events respectively. Note that events are here named E1, E2 ~~... consistent with Fig. **??** and also listed in~~ etc. consistent with Table A.

~~There is a minor tendency for the model to underestimate the SSA decrease and thus overestimate the predicted values of SSA as seen in Fig. 4b. Model limitations are most evident during the first day, as seen in Fig. 4, where the modelled decay consistently underestimates the magnitude of decrease. The model has limited ability to predict observations below in the lower range of SSA observations as seen in Fig. 4f, g and h, where the modelled and observed values are compared for each event.~~

~~Following our definition in Section 3.1 the eventshave an extent of 2-5 days. To assess model performance in predicting magnitude of SSA decrease for events of different time periods, we compare the predicted versus measured SSA~~ E9 in 2018 is poorly represented by the moderate-wind SSA decay model from this study. The mean air temperature for this event was -20.8 °C, 5 °C less than the next coldest (E11 at -15.3 °C). Fitting the model for E9 alone gives a decay rate of 0.44 m^2 kg^{-1} day^{-1}, similar that of the low-wind events. ~~For rapid events lasting 2-days the model tends to underestimate the rate of decrease. This is most apparent on Day 1 (24h after peak) for 2017 and 2018, while for 2019, Day 1 SSA is accurately predicted, with residuals increasing on Day 2. In comparison, events lasting 5-days show an underestimation for 2017 with negligible daily change in residuals, while the model overestimates~~ We therefore observe a temperature dependence of SSA decay similar to Cabanes et al. (2003). Based on limited number of events, we document low-winds having a similar effect to air temperatures below -20 °C on the SSA decay rate. Our results indicate a slower rate of decay under decreased wind-speed conditions. A similar effect is observed for low temperature, as the single SSA decay event in the moderate-wind category but with mean air temperature below -20 °C followed the decay rate of ~~E14 in 2018. However, field documentation suggests intermittent snow fall during Day 2 of E14, causing increase in SSA. Consideration for environmental context is explored in Section 2.5.1. E16 is characterised by~~ the ~~highest initial SSA values, and the largest residuals , suggesting the model is limited at very high initial SSA values.~~

~~The model requires only initial SSA as a parameter and predicts SSA decrease at EastGRIP within the defined conditions with an averaged~~ low-wind events.

3.2.1 Model evaluation

Table 2. *RMSE - Model comparison*

	Low-wind		Moderate-wind	
	Mean $m^2\,kg^{-1}$	Individual $m^2\,kg^{-1}$	Mean $m^2\,kg^{-1}$	Individual $m^2\,kg^{-1}$
This Study	3.64	4.76	2.48	3.50
FZ06	3.45	7.08	1.28	2.92
T07	6.34	7.11	5.63	6.10

This Study uses the respective α and C for the low- and moderate-wind events, using daily (mean) and individual samples. FZ06 parameters τ and n are defined by the look-up table from Flanner and Zender (2006). T07 uses the mean surface temperature for each event.

Model performance is tested by 1) comparing daily predicted decrease to the 10 daily observations, and 2) comparing results from this study to previous models from Flanner and Zender (2006) and Taillandier et al. (2007). Model-data residuals are normally distributed, suggesting no systematic errors in model predictions. The root mean squared error (RMSE) ~~of 5.6~~between model predictions and observed SSA is 4.76 $\mathrm{m^2\,kg^{-1}}$ ~~when considering all sample sites individually. The model predicts SSA decay over 2-5 day periods ($r^2 = 0.89$), with the highest RMSE of 6.17~~and 3.50 $\mathrm{m^2\,kg^{-1}}$ for ~~2019 compared to 4.97~~the low-wind and moderate-wind SSA decay events.

Using the physical-based decay model from Flanner and Zender (2006), hereafter referred to as FZ06, the influence of wind-speed on observed SSA decay rate can be assessed. Low-wind SSA decay events (E10 and E11) are most accurately predicted by FZ06 using the parameter values of $\tau =$ ~~m^2~~4.5 and n ~~kg^{-1} and 4.72~~= ~~$m^2\,kg^{-1}$ for 2017 and 2018 respectively. The model adequately predicts rapid SSA decay at EastGRIP within the temperature range, while for colder temperatures, the decay rate is the same but the intercept is significantly higher (Fig. 4a). Overall, for all included events during the three sampling years, behaviour of SSA decay is clearly captured by the model (Fig. 4c,d and e) . Exploring temperature conditions alone we find that the model performs well when daily mean surface temperatures are between -25 °C and 0 °C.~~ 6.1 from the look-up table (Flanner and Zender, 2006). Both the empirical model from this study, and the model from Taillandier et al. (2007), hereafter T07, underestimate the rate of decrease for low-wind decay events, most apparent during the first day of the event E10 (see Fig. A3).

3.2.2 ~~Environmental conditions during SSA decay events~~

~~Intuitively, environmental conditions would be considered to play a role for surface snow metamorphism and the rate of SSA decay . To explore this, hourly weather measurements from the PROMICE AWS and field report weather observations are analysed to provide environmental context to SSA decay events. Weather station data shows no systematic influence of basic~~

weather variables, relative humidity, surface temperature and wind speed on the model-data residuals, with linear regressions resulting in $r^2 < 0.1$ for all variables. An overview of event conditions using field observations are presented in Table A. Temperatures below -25°C are characterised by the same slope defined by the model (-0.54The data indicates that in natural conditions, wind-speed (between 6 $m^2 kg^{-1} day^{-1}$), but with a significantly higher intercept of 29 $m s^{-1} day^{-1}$ compared to 14.7and 7 $m s^{-1} day^{-1}$ for temperatures above -25) increases the surface SSA decay rate (α °C. Significant wind drift is expected when hourly mean wind speed exceeds 6= m-0.53, α s^{-1}, which happens during 144 days out of the total 258 sampling days from 2017, 2018 and 2019. Results indicate weather has no systematic influence on SSA decay during the first 2-5 days exposed at the surface, and that conditions vary for each event. The model is able to predict all defined decay events between -25= °C and 0 °C, indicating mechanisms of decay are the same. Daily mean values are more accurately predicted by the SSA decay model than individual sample sites due to snow surface variability. In-homogeneous surface snow is especially important to consider for isotopic composition, because there is potential for samples to contain snow from different precipitation and/or deposition events. -0.41). RMSE values presented in Table 2 indicate that FZ06 predicts decay with the least error, for both wind-speed categories. Moreover, all models have lowest errors when predicts events in the moderate-wind category.

3.2.2 Surface snow spatial variability

*Timeseries of snow isotopes and SSA*Timeseries of $\delta^{18}O$ (a), d-excess (b) and SSA (c) for 2017, 2018 and 2019 sampling seasons. d) shows the principle components of each parameter with colors corresponding to the color used to show absolute values. The black vertical lines indicate a break in the x-axis. Each faded line represents individual sample site values, and the thick line is the daily mean. Grey shaded regions indicate periods of high spatial variability in isotopic composition.

3.3 Isotopic change decay during events

The characterization of the SSA decays provide a basis to explore how snow metamorphism of surface snow plays a role for the alteration of isotopic composition of Greenland snow after deposition. A recent study at EastGRIP has shown the significant in-homogeneity in surface snow due to post-depositional reworking of the snow (Zuhr et al., 2021). The focus for this manuscript is to identify signal coherence between physical properties and isotopic composition of surface snow subject to precipitation/deposition and post-depositional processes. Autocorrelation analysis shows that isotopic composition values are spatially decorrelated after 10 m ($r^2 < 0.3$ after 10 m). Therefore, to avoid attenuation of isotopic signal, each sample is treated as independent. Isotopic composition is measured from each SSA sample containing snow from the top 2.5 cm of the snow surface , potentially containing snow deposition layers from multiple precipitation events. Surface heterogeneity is considered by using Empirical Orthogonal Function (EOF) analysis to determine the dominant mode of variance for each sampling year. Figure **??** shows timeseries of

The rate of change in SSA during low- and moderate-wind events is explored with respect to the rate of change in isotopic composition, given the covariance identified from EOF analysis. The rate of change in *d*-excess is plotted against the rate of change in SSA (Fig. 5), considering 1- and 2-day time intervals. We here include analysis of 2-day to allow isotopic

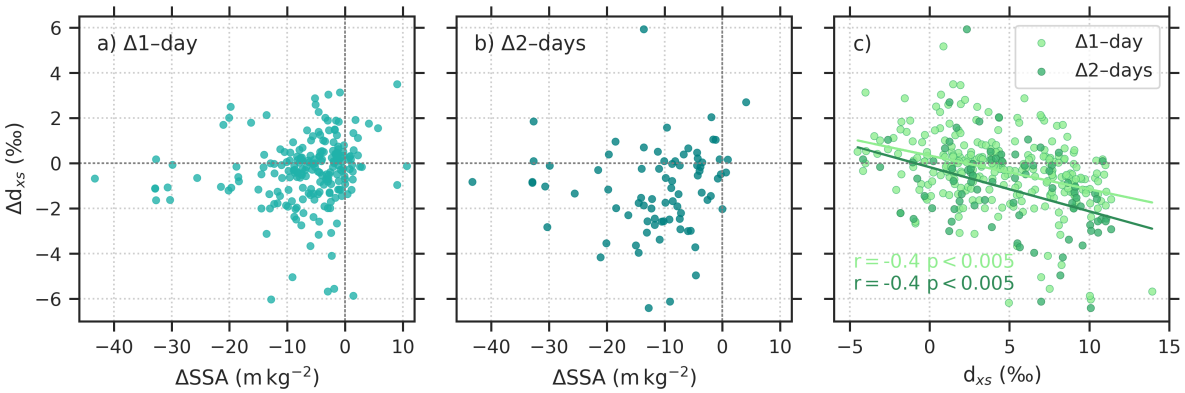

Figure 5. Isotopic change during all the analysed events are shown, with each point indicating a specific sampling site. The daily change in *d*-excess (d_{xs}) and SSA is presented in a), with 0 indicated with the grey dotted lines. The change in *d*-excess and SSA over a 2-day period is shown in b), while the change in *d*-excess is plotted against the absolute *d*-excess values is shown in c). Linear regressions are presented from daily change (light green) and 2-day change (dark green).

equilibration between the existing surface snow and snow deposited in the day preceding the event. The change after 2-days is presented in Table 3 for each low- and moderate-wind event.

All events have an overall change in isotopic composition, with the percentage change in *d*-excess being an order of magnitude higher than that of $\delta^{18}O$~~(a), d-excess (b) and SSA (c) with faded lines showing each sample site. The first principal components (PC1) of~~ . Increasing $\delta^{18}O$ ~~, d-excess and SSA are presented in Fig. **??**d. All parameters continuously change throughout the field seasons of 2017, 2018 and 2019. Isotopic composition measurements (Fig. **??**a, b) have larger spatial variability than SSA (Fig. **??**c).~~

~~Inter-annual variability is observed~~ corresponds to decreasing *d*-excess in 5 out of 8 events. E9, E11 and E13 deviate from this pattern. E9 and E13 both exhibit increases in $\delta^{18}O$ ~~, with seasonal mean values of -31.6‰, -32.7‰ and -27.3‰ for 2017, 2018~~ and ~~2019 respectively (Fig. **??**a). Note that the 2019 field season started approximately 15 days later than 2017 and 2018, resulting in a bias towards mid-summer conditions. Throughout the season~~ *d*-excess, whereas E11 is characterised by a slight decrease in $\delta^{18}O$ ~~follows a gradual increasing trend from May to August. Some cases of abrupt decreases (-10~~and ~~27%~~ decrease in *d*-excess.

Using a significance level of 0.05, the relationship between change in *d*-excess (Δ*d*-excess) and change in SSA (ΔSSA) is assessed. The results are presented in Fig. 7. Firstly, the Δ*d*-excess over 1-day are normally distributed around a mean of ~~-0.3‰) are observed in the late summer, for example at July 12th in 2018 and July 25th in 2019. No clear seasonal trend is observed in d-excess (Fig. **??**b) but with periods of gradual decreases. Total daily spread in $\delta^{18}O$ and d-excess is 15‰~~.

~~During 2017, 2018 and 2019 SSA has one dominant mode of variance (PC1) explaining 61~~Δ*d*-excess values ~~<%, 77-4%~~ and ~~72‰~~ tend to correspond to smaller ΔSSA (~~-15% of the total variance in the respective datasets. PC1 of $\delta^{18}O$ explains 69~~$m^2\,kg^{-1}$ ~~–0%, 83% and 75% of the total variance for the respective years. While PC1 of d-excess explains 47%, 51% and~~

60 % for 2017, 2018 and 2019 respectively. PC1 of δ^{18}O and d-excess show strong coherence from May to early June during 2017 and 2018, while for the second half of the season, and throughout 2019, PC1 of d-excess corresponds to PC1 of SSA (Fig. ??d)$m^2\,kg^{-1}$), suggesting that large decreases in *d*-excess occur after an extended period of exposure. This feature is highlighted in Fig.

Surface variability due to post-depositional reworking of the snow is shown by a wide spread in SSA values during a given day. Time periods with low spatial variability indicate largely homogeneous snow cover over the transect, shown in Fig. **??** as shaded regions. High variability is defined by periods where the 5-day running-mean of spatial variance in δ^{18}O is greater than one standard deviation. During periods of low spatial variability in isotopic composition, there is greater coherence between PC1 of SSA and PC1 of d-excess, due to a reduction of noise in the dataset. PC1 of SSA and d-excess show a coherence during 2018 and 2019 seasons, while the signal is less clear during 2017 7b, where *d*-excess decreases in 59 out of the 80 sites after two days of exposure to surface processes. Initial *d*-excess is observed to have a significant influence the magnitude of *d*-excess decrease over the defined period (Fig. **??**b). However, the reduced signal coherence is concurrent with high spatial variability in isotopic composition. 7c), with high initial *d*-excess corresponding to the largest decreases in *d*-excess.

A clear relationship between PC1 of SSA and PC1 of d-excess is observed when there is a relatively homogeneous snow layer over the sampling transect, defined by low spatial variance in δ^{18}O.

*Table of isotopic change for decay events*Behaviour

Table 3. Table of snow parameters during decay events are defined. The initial, 2-day and percentage isotopic change over a 2-day period are presented f

E1

E2

E3 -29.55 -30.07 -1.8% -0.2 -0.6 -200% 50.4 31.1 -38.3% **E4**

E5 -30.23 -29.88 1.2% 6.1 2.9 -52.5% 45.2 31.5 -30.2% **E6** -30.50 -30.36 0.5% 9.8 6.2 -36.7% 47.9 31.8 -33.6% **E8**

E10

E11

E12 -29.57 -29.33 0.8% 4.6 3.1 -32.6% 49.7 37.7 -24.1% **E13**

E14 -33.89 -34.26 -1.1% 11.5 12.3 7.0% 53.2 37.4 -29.7% **E15** -32.35 -31.94 1.3% 8.6 7.0 -18.6% 57.1 31.1 -45.6% **E16** -29.06 -28.97 0.3% 7.1 4.9 -3

E19 -23.40 -23.31 0.4% 6.7 6.8 1.5% 47.7 29.4 -38.2% **E20** -22.27 -22.26 0.1% 4.4 3.3 -25.0% 60.3 33.6 -44.2% **E21**

Behaviour of snow parameters during decay events are defined. The initial, 2-day and percentage change over a 2-day period are presented for δ^{18}O, *d*-e

3.3.1 Low-wind event analysis

3.3.2 Isotopic change during decay events

~~*Relationship between SSA and d-excess after the second day of each event*~~~~The relationship between the rate of change in SSA (ΔSSA $2days^{-1}$) and d-excess (Δd-excess $2days^{-1}$) over a 2-day period for a) individual samples for events presented in Table 3 for 2017 (o), 2018, (x) and 2019 (□), b) the same values colour coded by initial d-excess from each event. c) shows the relationship between change in d-excess after 2-days plotted against the initial d-excess value, with the linear regression line in black.~~

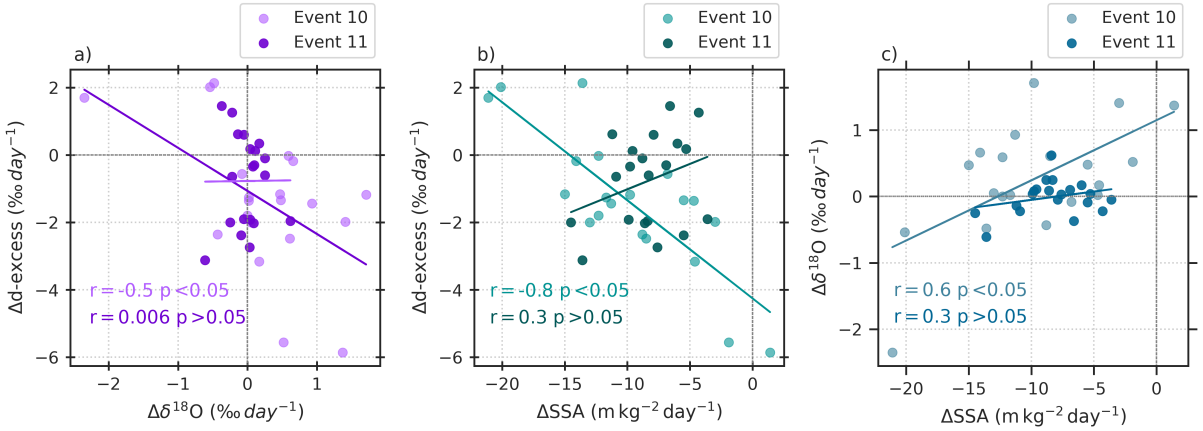

Figure 6. Isotopic change analysis for low-wind events, E10 and E11. Panel a) shows daily change in *d*-excess against change in d18O for E10 and E11 with corresponding linear regressions, b) shows change in *d*-excess against change in SSA, and c) shows change in d18O and change in SSA. The r- and p-value for each regression are indicating in the corresponding colours.

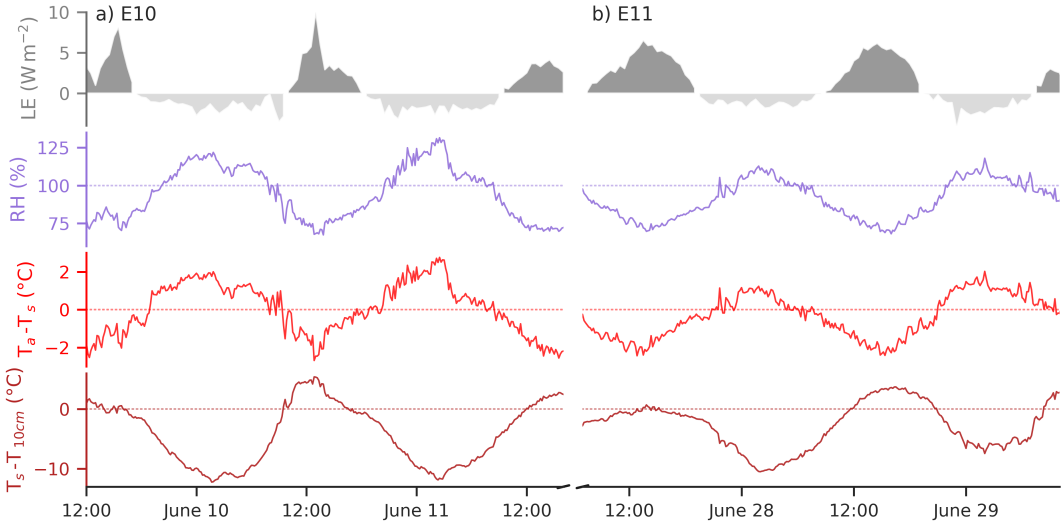

Figure 7. Latent heat flux (LE) (grey), relative humidity with respect to ice (purple), air-surface temperature gradient (TG) (red) and surface-10cm subsurface TG (red) for the low-wind SSA decay events, E10 (a) and E11 (b) (Table Dark grey shading in LE indicates sublimation and light grey shows deposition.

Using all 10 sample sites as independent values, the behaviour of isotopes during defined SSA decay events is analysed. To determine the isotopic change in the surface snow during rapid SSA decays, the rate of change in d-excess is plotted against the rate of change in SSA (Fig. 5). The change in SSA over a 2-day period is used. The daily mean change over the first 48h of each event is presented in Table 3.

In all events, the isotopic composition is observed to change, with δ^{18}O increasing after 2-days but mostly limited to As mentioned in section 3.1, ground fog preceded the SSA peak in E11, conccurent with negligible accumulation recorded. In contrast, approximately 1$\pm$1‰ mean increase, with the exception of E17 and E21 in 2019 (See Table 3). E17 is characterised by significant ground fog and snowfall during the event, while E21 has negative LHF (net-deposition) measured from the eddy-covariance system over the event. The percentage change of d-excess is an order of magnitude higher than $\delta^{18}O$ - expected due to the definition of d-excess - and similar to SSA , with 14 out of 19 events showing a decrease in d-excess during the first 2-days of each event. Further analysis looks specifically at the relationship between d-excess and SSA given the coherence observed between their PCs, and the significant change observed in Table 3. cm of snow was accumulated during the day prior to E10, corresponding to observation of snowfall.

SSA decreases by between 30 % and 53 % during the first 2-days, the largest change corresponding to the highest initial SSA value of 74 $m^2\,kg^{-1}$ as defined by the decay model. Using a significance level of 0.01, Figure 6 shows the relationship between change in d-excess after the second day of each event the daily change (Δd-excess) and change in SSA over the same time period (ΔSSA) is assessed. Events presented in Table 3 are shown in Fig. 7a. 72in isotopic composition and SSA. For E10, both $\Delta\delta^{18}$O and Δd-excess and ΔSSA and Δd-excess have significant negative correlations (r% of decreases in SSA correspond to decrease in d-excess when treating each sample as an independent value. All large decreases in SSA correspond to high SSA values, as the model describes. Increases in d-excess are observed at 12 samples sites, 6 of which are during 2017 and all correspond to initial d-excess values < 5=‰ (Fig. 7b) -0.5, r=-0.8). Thus suggests either low d-excess of deposited snow, or old snow that has been re-exposed. In addition, initial d-excess is observed to significantly influence that magnitude of d-excess change over the subsequent 48h of rapid SSA decay (Fig. 7a and b). The largest changes in d-excess corresponds to high initial d-excess values. Moreover, increases in d-excess during rapid SSA decay follow very low initial d-excess values. In summary, in 72Intuitively, $\Delta\delta^{18}$O and ΔSSA are positively correlated (r% (78 out of 108 samples) of cases decreases in SSA correspond to a decrease in d-excess of the snow sample during the first 2-days. Moreover, the magnitude of change in d-excess during rapid SSA decay shows a weak but significant dependence on the initial d-excess signal.

Significance of change in SSA and d-excess during events is tested by comparing the difference between the means of daily changes for event and non-event periods using a t-test with 0.01 significance level. Background variability in d-excess is 0.1$\pm$2.5=‰ for non-event periods, compared to -0.4$\pm$20.6), while no significant relationship is observed between the Δ-parameters during E11. All samples exhibit negligible change (<0.7‰for events alone. Similarly for SSA, non-events daily change is 0.04) in δ^{18}O during E11.

The dominant direction of vapour flux is assessed using air, surface and subsurface (10cm depth) temperature data and LE between the snow and atmosphere. Net-sublimation is observed during both E10 and E11, with a total sum of 33.9 $W\,m^{2-2}$ and 55.8 kg^{-1} compared to -7.7 $W\,m^{2-2}$ for the respective events. The LE is controlled primarily by the temperature gradient (TG)

between the air and the surface, with strong sublimation (>kg^{-1} for events. SSA decay events exhibit significant difference in distribution to non-event daily changes ($p < 0.01$, $t = 4.0070$, $df = 1715$, Std. Err. = 0.125). Moreover, changes in d-excess during events are double the magnitude of background variability with a consistently negative sign for all years, supporting evidence that d-excess of recently deposited snow has a 7210 % chance of decreasing during surface snow metamorphism (SSA decay) during the first two days, according to our data.

Analysis shows that rapid SSA decay events correspond to decreases in d-excess over a 2-day period in 72W % of the samples. Results from EOF analysis during periods of low spatial variance in isotopic composition over the sampling transect reveals a coherence between the dominant mode of variance of SSA and d-excess, suggesting that processes driving change in SSA also influence d-excess. m^{-2}), corresponding a negative TG between the air and surface of 2.5°C on June 10th. A concurrent upwards vapour flux is indicated based on the TG between the subsurface and surface snow. Downwards LE flux up to 4 W m^{-1} is observed each night corresponding to the transition from a negative to positive TG between the air and surface. The period between sampling on 9th June at 15:18 UTC and 10th June 10:40 UTC recorded net deposition, corresponding to significant increase in δ^{18}O and decrease in d-excess.

The amplitude of all parameters is during for E11 compared to E10. A negative surface-subsurface TG persists throughout the first day of E11, indicating a downwards vapour flux.

4 Discussion

Continuous daily SSA measurements at EastGRIP during the summer season of 2017, 2018 and 2019 have enabled quantification of variations in snow physical properties due to precipitation deposition and snow metamorphismduring summer. Understanding the relationship between rapid decreases in SSA and corresponding change in isotopic composition require clearly defined events and environmental context. Using a multi-day SSA decrease threshold, 21 events are defined from the summer field seasons of 2017, 2018 and 2019. All events are characterised by a peak and subsequent decay in SSA, the rate of which is proportional to the initial SSA value. set of criteria, nine SSA decay events during precipitation-free periods are defined and used to construct an empirical decay model. We firstly discuss the behaviour of SSA decay in precipitation free periods is driven by sublimationand vapour diffusion which is expected to influence the snow isotopic composition (Ebner et al., 2017; Hughes et al., 2021). decay at EastGRIP compared to existing models. The isotopic change associated with low-wind SSA decay events is then considered, in the context of sublimation, vapour diffusion and wind effects (Ebner et al., 2017; Hughes et al., 2021).

In this study , we present an empirical SSA decay model for surface snow of polar ice sheets based on continuous daily SSA measurements. The model describes SSA decay under natural summer conditions on the ice sheet. The findings from this study agree with previous studies, that SSA decay is most accurately at EastGRIP]Decay model developments

In this study , we present an empirical SSA decay model for surface snow of polar ice sheets based on continuous daily SSA measurements. The model describes SSA decay under natural summer conditions on the ice sheet. The findings from this study agree with previous studies, that SSA decay is most accurately at EastGRIP

The empirical decay model defined in this study accurately predicts the SSA decay of surface snow at EastGRIP over a limited time-period. We find that rapid SSA decay events are best described by an exponential ~~function (Cabanes et al., 2002), and indicates that the crystal structure of a new snow layer is a key driver of decay rate within the defined conditions over 2-5 day periods.~~

~~Comparison with weather station data showed that~~ decay function, in agreement with observations from Cabanes et al. (2003) . The expected temperature dependence on the SSA decay rate ~~during events had no systematic influence from weather variables (wind speed, temperature and relative humidity). The only exception is for temperatures outside the set range for the model. Surface temperatures below -25 °Cwere characterised by a significantly higher background SSA (defined as the mean SSA value of the final day of decay events) (Fig. 4), indicating high background SSA due to reduced snow metamorphism~~ is apparent during E9, where the mean air temperature is less than -20 °C, which is in agreement with the accepted knowledge that snow metamorphism is slower in colder conditions ~~. This observation is supported by theory and observation that~~ due to sublimation and deposition ~~are~~ being thermally activated processes ~~(Cabanes et al., 2003). Taillandier et al. (2007) (T07) developed an SSA decay model with a surface temperature parameter in addition to initial SSA which is able to capture the behaviour of decay during the cold event, E7, at EastGRIP suggesting temperature is important to consider when predicting SSA outside the defined temperature range. However,~~ (Cabanes et al., 2003; Legagneux et al., 2003; Flanner and Zender, 2006; Taillandier et al., 2007) . The narrow temperature range of SSA decay events does not facilitate a conclusive definition of a temperature-dependent decay rate.

In addition, we focus on the influence of ~~temperature on~~ wind-speed of the SSA decay rate ~~within the defined temperature range is negligible. Model-observation comparisons show equal performance for the SSA decay model from this study (r^2 = 0.89) compared to T07 temperature gradient metamorphism model (r^2 = 0.9).~~ and observe a more rapid SSA decay with increased wind-speed, potentially due to increased ventilation of saturated pore air acting as a catalyst for snow metamorphism (Cabanes et al., 2003; Flanner and Zender, 2006; Neumann and Waddington, 2004). Wind erosion cannot be definitively ruled out due to dis-continuous documentation of surface conditions. However, in some cases, high wind speeds are documented to increase SSA due to fragmentation and sublimation of suspended snow grains, which are then re-deposited and effectively sieved into the pore spaces of the surface snow layer (Domine et al., 2009).

~~The top 1 cm of the 2.5 cm SSA sample is measured by the Ice Cube device, and thus, is most likely to capture the precipitation signal (Gallet et al., 2009; Klein, 2014). Directly after precipitation, isothermal snow metamorphism is expected to be dominant due to to high surface curvature of fresh snow crystals (Colbeck, 1980). Alternative SSA decay models are proposed by Taillandier et al. (2007) to describe snow metamorphism under temperature gradient (temperature driven recrystallisation) and isothermal (curvature driven recrystallisation) metamorphism, with the surface temperature and initial SSA being variable parameters.~~ Comparison to existing physical models allows for the assessment of the additional influence of wind-speed, not considered previously (Flanner and Zender, 2006). However, we find that ~~all events are most accurately predicted using the temperature gradient decay equation, which accounts for the very low surface temperature observed in E7. The similarity in prediction for -25 °C to 0 °C suggests the EastGRIP SSA decays are not only driven by crystal curvature but by temperature gradient vapour diffusion as well.~~

~~The influence of snow metamorphism after precipitation during winter is expected to be reduced due to low temperatures and negligible temperature gradients during polar night. Based on this, the model is only recommended to use for polar ice sheet summer conditions only. Within the defined conditions,~~ FZ06 most predicts the moderate-wind events with the lowest error. This is potentially due to the ~~SSA decay model is a simple empirical model~~ initial conditions for low-wind event E10 likely corresponding to surface hoar, while the models from the literature tend to describe SSA decay ~~in the accumulation regions of the Greenland Ice Sheet, with dependence on the initial SSA alone.~~ from precipitation. The initial SSA value of $46\,m^2\,kg^{-1}$ for E10 is in agreement with documented SSA of surface hoar (Domine et al., 2009).

4.1 ~~Decay model applications~~

~~Conditions for the model are expected to be applicable over the Greenland Ice Sheet interior under mean summer conditions. The model predicts decay events at EastGRIP with a r^2 of 0.89, compared to observation, within defined conditions. SSA estimates from satellites have previously been compared to ground observations and show a strong correlation between daily mean SSA and satellite retrieved SSA at EastGRIP (Kokhanovsky et al., 2019). The SSA decay model has the potential to predict SSA decay~~ Modelling SSA decay using continuous in-situ measurements is associated with a number of limitations relating to surface perturbation by the wind and hoar formation, but nevertheless, is vital for studying surface energy balance and post-depositional change in isotopic composition. To test the model over the entire accumulation zone of the ~~Greenland Ice Sheet~~ GIS using satellite data ~~, the model can be evaluated for different sites to document the spatial variability in SSA over the entire ice sheet, and describe the summer SSA decay. This has additional benefits for quantification of surface mass balance and surface energy budget due to the relationship between snow microstructure and surface albedo.~~ following the methods in Kokhanovsky et al. (2019) would be an interesting future study, but is outside the scope of this manuscript.

4.1 ~~Rapid SSA decay and d-excess~~Inter-annual variability

~~In this study, processes driving snow metamorphism are documented to influence isotopic composition of the snow after precipitation, supporting experimental observations and theoretical understanding (Ebner et al., 2017; Wahl et al., 2021; Hughes et al., 202 . Results from this study suggest that surface snow metamorphism following precipitation eventscorresponds to change in isotopic composition, most clearly observed in d-excess (Table 3)~~The surface snow over the 90 m sampling transect is often non-homogeneous due to uneven distribution of accumulation. EOF analysis is used to account for spatial variability at each site, and to determine covariance between the parameters SSA, $\delta^{18}O$ and d-excess. The positive mode of $PC1_{SSA}$ is associated with depositional events, such as precipitation, surface hoar formation, and wind-fragmented snowdrift, causing an increase in SSA (Domine et al., 2009), while the negative mode is associated with snow metamorphism or wind scouring (Cabanes et al., 2002, 2003; Legagneux et al., 2003, 2004; Taillandier et al., 2007; Flanner and Zender, 2006). Based on ~~our results, rapid decreases in SSA correspond to decreases in d-excess of a new snow layer in 72 % of cases during the first 2-days of rapid SSA decay.~~ this interpretation, correlations between $PC1_{SSA}$ and $PC1_{d-excess}$ or $PC1_{\delta^{18}O}$ suggests the aforementioned mechanisms controlling SSA variability also influence the isotopic composition.

~~Using the eddy-covariance latent heat flux measurements, we observed net sublimation during all decay events(with the exception of E21) used for isotopic analysis, which is in agreement with recent studies that document fractionation during sublimation results in slight increases~~

Accumulation intermittency and temperature conditions are proposed as a potential explanation for the change in regime from a coherence between $PC1_{\delta^{18}O}$ and $PC1_{d-excess}$ in 2018 and $PC1_{SSA}$ and $PC1_{d-excess}$ in ~~$\delta^{18}O$ and decreases in d-excess (Madsen et al., 2019; Hughes et al., 2021; Wahl et al., 2021). However, sublimation is not the only process occurring. Vapour pressure gradients due to surface curvature drive snow metamorphismvia vapour diffusion through the pore space and thus, kinetic fractionation is expected to influence the isotopic composition. A larger influence is expected for d-excess than $\delta^{18}O$ because kinetic fractionation influences δD more than $\delta^{18}O$ ($d - excess = \delta D - 8 \cdot \delta^{18}O$) with a stronger influence on d-excess than $\delta^{18}O$, which can explain the covariance between d-excess and SSA observed most clearly during 2019 (Cappa et al., 2003; Da . Our approach to~~ 2019. Casado et al. (2021) show that during low precipitation periods in Antarctica, the isotopic signal is strongly modified during snow metamorphism. Approximately 10 cm of accumulation is recorded in both 2018 and 2019, but a gradual increase during 2018 suggests multiple small deposition events, whereas 2019 is characterised by step-like increases. Therefore, the ~~change over a 2-day period instead of daily change allows for increased propagation of the isotope signal during SSA decay to account for the 1~~strong correlation between $PC1_{SSA}$ and $PC1_{d-excess}$ can be attributed to increased surface exposure and warmer temperatures facilitating snow metamorphism, in agreement with findings from Casado et al. (2021).

Low accumulation during 2017 presents a caveat to this interpretation, with results from 2017 showing $PC1_{d-excess}$ to be influence by both $PC1_{SSA}$ and $PC1_{\delta^{18}O}$ during different periods. The period from May 15th to June 10th follows the regime observed during 2018 and corresponds to a negligible temperature gradient between the air, surface, and 10 ~~cm representation from Ice Cube SSA measurements, compared to the 2.5~~cm ~~bulk isotope measurements (Gallet et al., 2009; Klein, 2014). A significant relationship is observed between change in d-excess and change in SSA during the first 2-days compared to daily analysis (with an additional relationship observed during 2019 between daily change in d-excess and daily change in SSA). Decreases in d-excess are observed during rapid SSA decay, driven by a combination of sublimation, deposition and vapour diffusion through the pore space.~~

~~Surface snow metamorphism is not confined to rapid SSA decreases, and thus isotopic compositionchange is observed continuously. However, results from this study indicate that d-excess changes during rapid SSA decay have significantly different distribution than the background non-event fluctuations. Our findings are in agreement with a study from Antarctica which showed a significant relationship between d-excess and physical snow properties with depth, while negligible relationship was observed for δ^{18}O (Dadic et al., 2015). Our study has selected rapid SSA decays fitting to~~ subsurface (Fig. A4). In contrast, the period from July 1st onwards is characterised by a near-constant upwards vapour flux, indicated by a negative temperature gradient between the ~~decay model to address how changes in snow crystal morphology after precipitation relates to change in isotopic composition. Future studies would benefit from using isotope flux models to account for the influence of sublimation and deposition, to determine unexplained isotopic composition change~~ air, surface, and subsurface. $PC1_{d-excess}$ covaries with $PC1_{SSA}$ during this period, much like 2019, suggesting that vapour diffusion driven by temperature gradients modifies the

snow isotopic composition. This agrees with previous studies documenting kinetic effects during snow grain growth resulting from pore space diffusion (Neumann and Waddington, 2004; Casado et al., 2016; Ebner et al., 2017; Casado et al., 2021).

~~An additional feature supporting the observation of processes driving surface snow metamorphism corresponds to a decrease in d-excess, is a clear relationship between substantial increases in SSA and increase in d-excess (Fig. ??) . The upper 10th percentile of ΔSSA increases ($14.7\,m^2\,kg^{-1}$) corresponds to positive Δd-excess in 70 % of cases (Fig. 7). Large increases in SSA are closely associated with precipitation, however, increases are observed in~~ The opposing phases of the North Atlantic Oscillation (NAO) between the years can explain the different meteorological conditions. The NAO is in a ~~number of other scenarios (Domine et al., 2009). Precipitation is expected to cause the largest SSA, suggesting that the d-excess of precipitation is most often higher than existing surface snow. Our results therefore suggest that the precipitation isotopic composition signal is not always preserved after snow metamorphism due to (kinetic) fractionationduring sublimation and other surface processes.~~ positive phase during 2018 and the majority of 2017 bringing below-average temperatures, as observed at EastGRIP (Hanna et al., 2015). The opposite is observed during 2019, corresponding to a positive phase in the NAO.

~~*Change in d-excess per day (Δd-excess* day^{-1}*) vs. change in SSA per day (ΔSSA*day^{-1}*)*~~~~The relationship between the rate of change in SSA per day (ΔSSAday^{-1}) and d-excess (Δd-excessday^{-1}) for all summer seasons 2017-2019 (light grey), all events (dark grey) and selected events based on substantial accumulation (dark turquoise). The box indicates the values corresponding to daily decrease in d-excess during decrease in SSA, with 81 % of selected events in this quadrant.~~ Conclusive results from EOF analysis are limited by wind-effects, especially in the negative phase, corresponding to decrease in SSA, where wind scouring potentially removes the surface layer (Domine et al., 2009; Flanner and Zender, 2006; Hachikubo et al., 2014) . Decoupling snow metamorphism from wind scouring is considered in the following section on isotopic change during low-wind SSA decay events.

4.2 ~~Influence of event conditions on isotopic change~~

~~Surface conditions prior to and~~

4.2 Isotopic change during SSA decay events

Three key mechanisms are expected to drive the rapid SSA decays, 1) large grains growing at the expense of small grains (Legagneux et al., 2004; Flanner and Zender, 2006), 2) diffusion of interstitial water vapour (Colbeck, 1983; Ebner et al., 2017; Touzeau et , 3) sublimation due to the wind ventilating the saturated pore air, known as 'wind-pumping' (Neumann and Waddington, 2004; Town et al., . The dominant mechanisms can theoretically be identified by a combination of the change in isotopic composition - indicating the fractionation effect - and the LE and temperature gradient data.

In theory, mechanism 1) causes minimal change in the bulk isotopic composition of a snow layer under isothermal conditions (Ebner et al., 2017). Therefore, observations of SSA decay corresponding to negligible isotopic composition change could be explained by this mechanism. We observe no events with consistent isotopic composition throughout. In the instance of 2) interstitial diffusion, light isotopes are preferentially diffused, while the heavy isotopes will be preferentially deposited onto the cold snow grains (Colbeck, 1983; Ebner et al., 2017; Touzeau et al., 2016). Thus, diffusion of water vapour in the

pore space causes a decrease in d-excess and slight increases in δ18O due to kinetic fractionation (Flanner and Zender, 2006) . 3) Sublimation has been widely documented to cause an increase in δ^{18}O of the remaining snow-mass due to equilibrium fractionation, and a significant decrease in d-excess due to kinetic fractionation (Ritter et al., 2016; Madsen et al., 2019; Hughes et al., 2021 .

An overall increase in δ18O and decrease in d-excess during E10 can be attributed to a combination of 2) and 3) based on observation of net-sublimation and high amplitude diurnal temperature gradient variability indicating vapour transport within the pore space. The period between 9th June at 15:18 UTC and 10th June 10:40 UTC recorded net deposition corresponding to an overall decrease in δ18O during ~~SSA decay events vary, with a number of events having no measured accumulation or observed snowfall (Fig. **??**) . Removing events with non-homogeneous increases in surface height and events where additional precipitation or significant snowdrift are observed, reveals that during rapid SSA decays following significant precipitation, there is increased likelihood of observing concurrent decrease in d-excess during~~ the first day ~~(Fig. **??**). This observation combined with results presented in Fig. 7a strongly suggests that initial snow metamorphism after precipitation~~ and minimal decrease in d-excess, potentially due a deposition of atmospheric water vapour (Stenni et al., 2016; Feher et al., 2021; Casado et al., 2021) .

A 30% decrease in d-excess corresponds to a ~~decrease in d-excess of in the surface snow.~~ negligible change in δ18O during E11. Net-sublimation double that of E10 is measured, but with reduced amplitude in both TGs. Moreover, the largest decrease in d-excess occurs after the first day when the surface-subsurface TG is consistently negative, indicating that vapour diffusion plays a role in modifying the isotopic composition, and the effect of equilibrium fractionation during sublimation from the surface only weakly influences the bulk isotopic composition over the 3-day period (Casado et al., 2021). Decoupling the influence of atmosphere-surface exchange and diffusion from subsurface snow requires additional measurements of isotopic composition of atmospheric water vapour and precipitation isotopes, which is outside the scope of this study.

4.3 ~~Spatial variability of snow surface~~

~~Low accumulation rates at EastGRIP result in the potential for winter snow layers to influence the isotopic composition in the 2.5 cm surface snow. Accumulation heterogeneity causes uneven mixing of layers at each sample site, which is observed clearly in the large spatial variability in isotopic compositionmeasurements in Fig. **??**a and b. EOF analysis is used to account for spatial variability at each site, and a coherence is observed between the principal components of d-excess and SSA. PC1 is weaker when spatial variability is high, and during these periods the coherence between d-excess and SSA are muted. During the start of 2017 and 2018 PC1 of d-excess is coherent with PC1 of $\delta^{18}O$, and decoupled from PC1 of SSA. At the start of the season, the 2.5 cm sample will contain winter snow layers which are less influenced by snow metamorphism (Libois et al., 2015; Town et al., 2008), and thus, a coherent signal between d-excess and $\delta^{18}O$ is observed. The transition to a coherence between PC1 of d-excess and PC1 of SSA can be explained by summer snow layers, influenced by snow metamorphism, causing d-excess to appear to become decoupled from $\delta^{18}O$, which is less influenced by kinetic fractionation than δD (Masson-Delmotte et al., 2005) during snow metamorphism.~~

4.3 ~~Implications to ice core interpretation~~

4.3 Implications and perspectives

~~Documented changes in snow isotopic composition during surface snow metamorphism have potential implications for interpretation of stable water isotope records from ice cores, given that the current interpretation assumes the precipitation signal is preserved (Dansgaard, 1964). Seasonal transition from a coupling of PC1~~ Our results suggest that processes driving snow metamorphism modify the isotopic composition of ~~d-excess and PC1 of δ^{18}O, to a coherence between PC1 of d-excess PC1 of SSA at the latter part of the season, suggest that summer snow metamorphism causes d-excess to appear to decouple from δ^{18}O. Kinetic fractionation during sublimation~~ the snow while exposed at the surface, supporting experimental observations and theoretical understanding (Ebner et al., 2017; Wahl et al., 2021; Hughes et al., 2021). We find that *d*-excess is mostly influenced by vapour fluxes in the pore space, driven by temperature gradients. Net-sublimation appeared to have less influence on the isotopic composition, but this is expected to be ~~the cause a decrease in d-excess in the snow, given the different diffusivities of HDO and and $H_2{}^{18}O$ (Masson-Delmotte et al., 2005).~~ due to the depth of the sample and the short duration of both low-wind events.

~~Seasonal signals are influenced by millennial scale insolation variability (Masson-Delmotte et al., 2006; Laepple et al., 2011) . An inverse relationship is observed between obliquity and d-excess over the past 250ka years at Vostok which is attributed to the insolation gradient between high and low latitudes causing increases moisture transport from low latitudes relative to high latitudes (Vimeux et al., 2001, 1999). Results presented in our study document decreases in snow d-excess during surface snow metamorphism . Millennial scale local insolation variability has a strong influence on temperature gradients in the snow (Hutterli et al., 2009). Thus, it is possible that local insolation variability may also influence d-excess due to temperature gradients in the snow driving snow metamorphism at the surface .~~

~~Our results highlight the need to consider the influence of surface snow metamorphism on isotopic composition in stable water isotope records as the traditional interpretation of d-excess ice core signal does not account for any post-depositional signal.~~ The findings of this exploratory study reiterates the importance of quantifying the isotopic fractionation effects associated with processes driving snow metamorphism during precipitation free periods. Moreover, the inter-annual variability observed at EastGRIP between 2018 and 2019 suggests that precipitation intermittency and temperature (gradients) play a role in isotopic change, which is not so readily identified in the surface snow SSA data. Future work to decouple the processes driving change in ~~d-excess~~ *d*-excess (sublimation from surface or interstitial vapour diffusion in the pore space) is vital for modelling the change in isotopic composition down to the close-off depth in the firn (Touzeau et al., 2018; Neumann and Waddington, 2004). ~~In addition, it would be beneficial to obtain~~ Future studies would benefit from obtaining direct measurements of the isotopic composition ~~and SSA of precipitation~~ of precipitation and surface hoar, to determine the fraction of ~~precipitation~~ such deposits in the SSA samples. Furthermore, a quantitative representation of vapour fluxes in the surface snow would provide a basis from which to quantify the the relative influence of fractionation during sublimation and interstitial diffusion.

5 Conclusions

This study addresses the rapid SSA decay driven by surface snow metamorphism. In particular, the study aims to explore how rapid SSA decay relates to changes in isotopic composition of the surface snow in the dry accumulation zone of the Greenland Ice Sheet. Ten individual snow samples were collected on a daily basis at EastGRIP in the period between May and August of 2017, 2018 and 2019. SSA and isotopic composition was measured for each sample. Periods of snow metamorphism after precipitation deposition events are defined using SSA measurements to extract periods of rapid decreases in SSA.

An exponential SSA decay model (~~$SSA(t) = (SSA_0 - 26.8)\,e^{-0.54t} + 26.8$~~ $SSA(t) = (SSA_0 - C)\,e^{-\alpha \cdot t} + C$) was constructed to describe surface snow metamorphism under mean summer conditions for polar snow, with surface temperatures ~~between -25~~above -30 °C~~and 0 °C and wind speeds below 6 $m\,s^{-1}$. The empirical model can be applied to remote areas of polar ice sheets and requires only initial SSA as the parameter, making it simple to use~~. Two categories were defined to assess the influence of wind-speed on the SSA decay rate. The relationship between defined events of snow metamorphism and corresponding snow isotopic composition was then explored.

~~We observe changes~~ Changes in isotopic composition corresponding to post-depositional processes driving ~~rapid SSA decay . Principal components from EOF analysis for SSA and d-excess indicate that under near-homogeneous surface snow conditions, d-excess varies in phase with SSA throughout a large proportion of the sampling seasons. This suggests that post-depositional processes and precipitation influence both physical snow structure and isotopic composition concurrently.~~ SSA decay is observed in all events. Over the first ~~2-days of rapid~~ 2 –days of SSA decay events, ~~d-excess~~ *d*-excess is observed to decrease ~~significantly~~ from the initial~~value for most events , at the same time we observe net sublimation. Significant changes in surface snow d-excess are observed during days following a precipitation event, suggesting that precipitation d-excess signal is altered after deposition, together with changes in physical snow properties (SSA).~~ . Analysis of SSA decay events with consistent low wind speed indicates that the combined effects of vapour diffusion and diurnal LE variability causes isotopic fractionation of the surface snow in the absence of precipitation.

In summary, our results suggest that the precipitation isotopic composition signal is not always preserved due to isotopic fractionation during the processes driving surface snow metamorphism. Observations of post-depositional decrease in ~~d-excess~~ *d*-excess during rapid SSA decay hints to local processes influencing the ~~d-excess~~ *d*-excess signal and therefore an interpretation as source region signal is implausible.

Appendix A

Table A1. *SSA Decay Event Conditions*Duration and conditions for all 21 events defined by the threshold. 'Initial Conditions' refers to the conditions during the day (24h) before the event, while 'SSA Decay Event Conditions' describes the dominant conditions for the event duration, based on field observations. 'Surface Temperature' is the mean surface temperature during the event. 'Comments' highlight any significant weather behaviour during the event.

	Date	Event No.	Surface Temperature	Initial Conditions	Event Conditions	Comments
2017	27/05 - 01/06	E1	-17.3	No clear driver	Clear-sky	
	19/06 - 24/06	E2	-13.6	Snowfall	Clear-sky	
	30/06 - 02/07	E3	-14.0	Snowfall	Overcast	Snow drift Day-0
	10/07 - 15/07	E4	-13.2	Snowfall	Clear-sky	
	18/07 - 19/07	E5	-11.7	Snowfall	Overcast	
	21/07 - 23/07	E6	-11.2	Snowfall	Overcast	
2018	07/05 - 10/05	E7	-33.7	Drift and fog	Clear/ice-fog	Snowfall Day-2
	14/05 - 15/05	E8	-19.8	Snowfall	Clear-sky	
	16/05 - 18/05	E9	-21.5	Snowfall and fog	Overcast	
	09/06 - 11/06	E10	-14.9	Ground fog	Overcast	
	27/06 - 29/06	E11	-15.3	Ground fog	Clear-sky	
	30/06 - 03/07	E12	-11.2	Wind drifted snow	Clear-sky	
	04/07 - 06/07	E13	-10.2	Snowfall	Clear-sky	
	16/07 - 21/07	E14	-14.3	No clear driver	Clear-sky	Dusting of snow
	23/07 - 27/07	E15	-14.1	Ground fog	Clear-sky	
2019	17/06 - 20/06	E16	-11.4	Snowfall	Clear-sky	
	27/06 - 30/06	E17	-9.5	No clear driver	Overcast	Fog and snow
	02/07 - 05/07	E18	-7.0	Snowfall	Overcast	
	06/07 - 08/07	E19	-10.0	No clear driver	Clear-sky	
	18/07 - 20/07	E20	-7.6	Ground fog	Overcast	
	28/07 - 31/07	E21	-6.5	No clear driver	Clear-sky	

Duration and conditions for all 21 events defined by the threshold. 'Initial Conditions' refers to the conditions during the day (24h) before the event, while 'Event Conditions' describes the dominant conditions for the event duration, based on field observations. 'Surface Temperature' is the mean surface temperature during the event. 'Comments' highlight any significant weather behaviour during the event.

*Accumulation at each sample site*Accumulation measurements from each sample site over the 90 m sampling transect is shown here for 2017, 2018 and 2019 respectively. Each line represents an individual site. Negative values indicate a decrease in surface height, and positive values suggest precipitation or deposition adding to the surface height. The grey bars show the individual events defined in Section 3.1

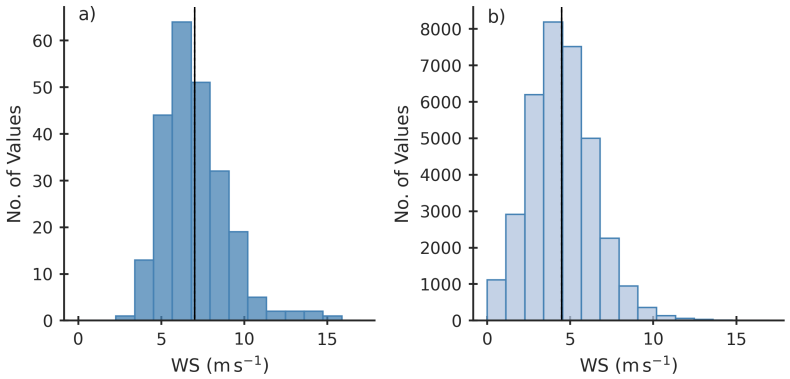

Figure A1. *Wind-speed Distribution*

Histograms showing a) the daily maximum values and b) the 10-minute mean values for all sampling days of 2017, 2018 and 2019. The black line indicates the mean.

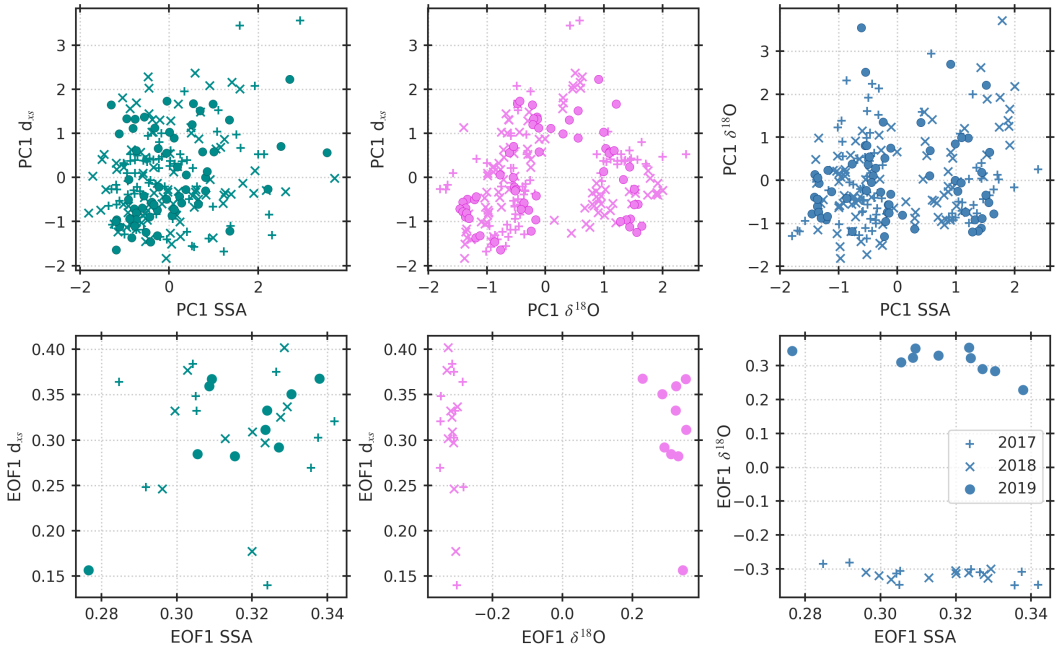

Figure A2. *EOF analysis*

Data availability. The SSA, density and accumulation data for all sampling years is available on the PANGAEA database with the DOI:***. Snow isotope data is also available on the PANGAEA database with the DOI:***. Data from the Programme for Monitoring of the Greenland

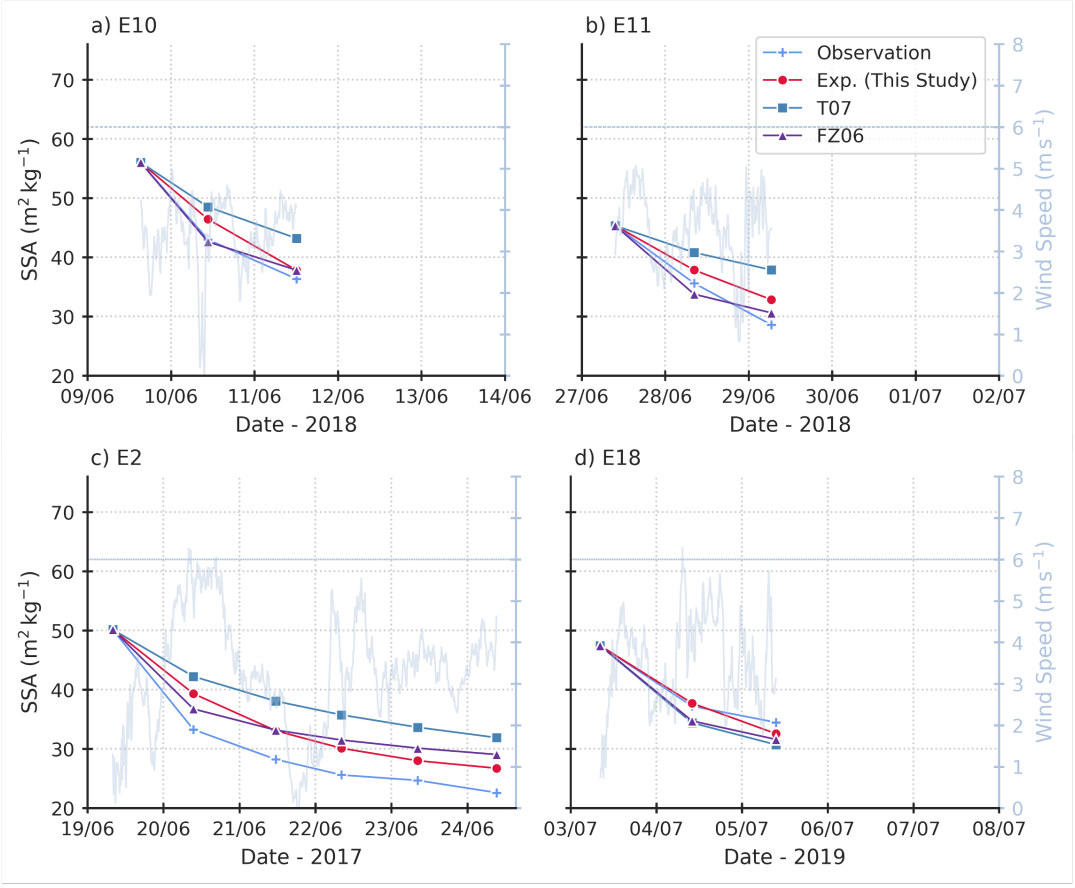

Figure A3. *Decay Model Construction and Predictions*

A comparison between the observations, the decay models from this study and the existing decay models from Flanner and Zender (2006), FZ06, and Taillandier et al. (2007), T07. The 10-minute averaged wind-speed is shown on the secondary y-axis, with the 6 ms-1 thresholds indicated. The low wind events E10 and E11 are shown in a) and b), and examples of two moderate-wind events are show in c) and d).

Ice Sheet (PROMICE) 400 were provided by the Geological Survey of Denmark and Greenland (GEUS) at http://www.promice.dk. Eddy Covaraniance Tower measurement are available on the PANGAEA database with the DOI: https://doi.org/10.1594/PANGAEA.928827.

Author contributions. HCSL, AKF and RHS designed the study together. AKF, SW, MH, MB, AZ, SK and HCSL carried out the data collection and measurements. RHS, AKF and HCSL worked directly with the data. RHS, AKF and HCSL prepared the manuscript with contributions from all co-authors. AKF contributed largely to the manuscript text and structure. HCSL designed and administrated the SNOWISO project.

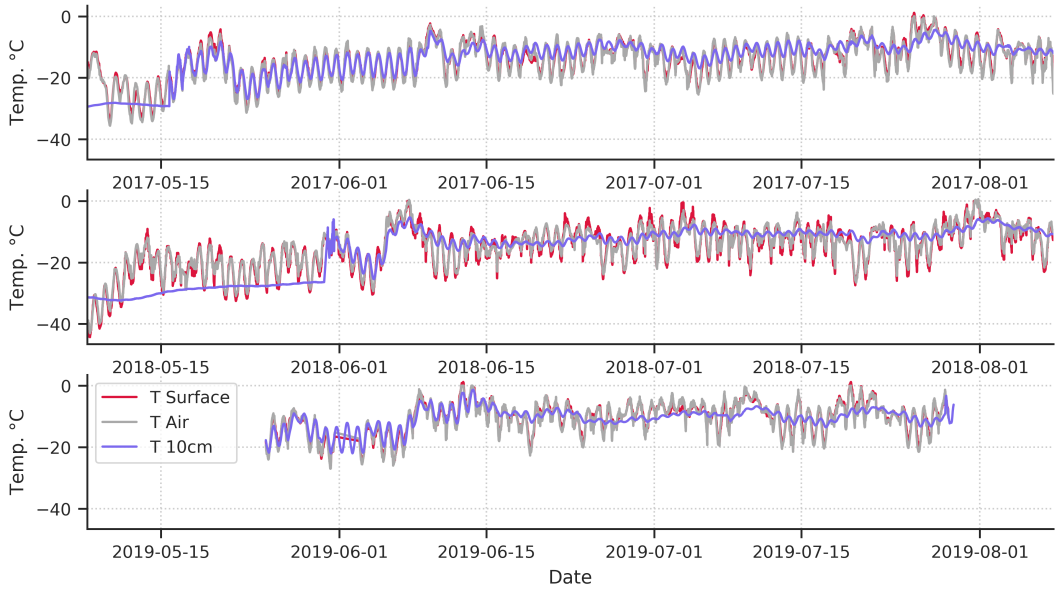

Figure A4. *Air, surface and subsurface temperature time-series*

Competing interests. The authors declare that they have no conflict of interest.

Acknowledgements. This project has received funding from the European Research Council (ERC) under the European Union's Horizon 2020 research and innovation program: Starting Grant-SNOWISO (grant agreement 759526). EastGRIP is directed and organized by the Centre for Ice and Climate at the Niels Bohr Institute, University of Copenhagen. It is supported by funding agencies and institutions in Denmark (A. P. Møller Foundation, University of Copen-hagen), USA (US National Science Foundation, Office of Polar Programs), Germany (Alfred Wegener Institute, Helmholtz Centre for Polar and Marine Research), Japan (National Institute of Polar Research and Arctic Challenge for Sustainability), Norway (University of Bergen and Bergen Research Foun-dation), Switzerland (Swiss National Science Foundation), France (French Polar Institute Paul-Emile Victor, Insti-tute for Geosciences and Environmental research), and China (Chinese Acad-emy of Sciences and Beijing Normal University).

References

Birnbaum, G., Freitag, J., Brauner, R., Ko¨nig, G., Ko¨nig-Langlo, K., Schulz, E., Kipfstuhl, S., Oerter, H., Reijmer, C. H., Schlosser, E., Faria, S. H., Ries, H., Loose, B., Herber, A., Duda, M. G., Powers, J. G., Manning, K. W., and Van Den Broeke, M. R.: Strong-wind events and their influence on the formation of snow dunes: observations from Kohnen station, Dronning Maud Land, Antarctica, Journal of Glaciology, 56, 891–902, https://www.cambridge.org/core., 2010.

Cabanes, A., Legagneux, L., and Dominé, F.: Evolution of the specific surface area and of crystal morphology of Arctic fresh snow during the ALERT 2000 campaign, Atmospheric Environment, 36, 2767–2777, https://doi.org/10.1016/S1352-2310(02)00111-5, 2002.

Cabanes, A., Legagneux, L., and Dominé, F.: Rate of evolution of the specific surface area of surface snow layers, Environmental Science and Technology, 37, 661–666, https://doi.org/10.1021/es025880r, 2003.

Cappa, C. D., Hendricks, M. B., DePaolo, D. J., and Cohen, R. C.: Isotopic fractionation of water during evaporation, Journal of Geophysical Research: Atmospheres, 108, https://doi.org/10.1029/2003jd003597, 2003.

Carmagnola, C. M., Domine, F., Dumont, M., Wright, P., Strellis, B., Bergin, M., Dibb, J., Picard, G., Libois, Q., Arnaud, L., and Morin, S.: Snow spectral albedo at Summit, Greenland: Measurements and numerical simulations based on physical and chemical properties of the snowpack, Cryosphere, 7, 1139–1160, https://doi.org/10.5194/tc-7-1139-2013, 2013.

Casado, M., Cauquoin, A., Landais, A., Israel, D., Orsi, A., Pangui, E., Landsberg, J., Kerstel, E., Prie, F., and Doussin, J. F.: Experimental determination and theoretical framework of kinetic fractionation at the water vapour-ice interface at low temperature, Geochimica et Cosmochimica Acta, 174, 54–69, https://doi.org/10.1016/j.gca.2015.11.009, 2016.

Casado, M., Landais, A., Picard, G., Münch, T., Laepple, T., Stenni, B., Dreossi, G., Ekaykin, A., Arnaud, L., Genthon, C., Touzeau, A., Masson-Delmotte, V., and Jouzel, J.: Archival processes of the water stable isotope signal in East Antarctic ice cores, Cryosphere, 12, 1745–1766, https://doi.org/10.5194/tc-12-1745-2018, 2018.

Casado, M., Münch, T., and Laepple, T.: Climatic information archived in ice cores: Impact of intermittency and diffusion on the recorded isotopic signal in Antarctica, Climate of the Past, 16, 1581–1598, https://doi.org/10.5194/cp-16-1581-2020, 2020.

Casado, M., Landais, A., Picard, G., Arnaud, L., Dreossi, G., Stenni, B., and Prié, F.: Water Isotopic Signature of Surface Snow Metamorphism in Antarctica, Geophysical Research Letters, 48, https://doi.org/10.1029/2021GL093382, 2021.

Christiansen, H. H.: Snow-cover depth, distribution and duration data from northeast Greenland obtained by continuous automatic digital photography, Annals of Glaciology, 32, 102–108, https://www.cambridge.org/core., 2001.

Ciais, P. and Jouzel, J.: Deuterium and oxygen 18 in precipitation: Isotopic model, including mixed cloud processes, Tech. Rep. D8, 1994.

Colbeck, S. C.: THERMODYNAMICS OF SNOW METAMORPHISM DUE TO VARIATIONS IN CURVATURE, Journal of Glaciology, 26, 291–301, https://www.cambridge.org/core., 1980.

Colbeck, S. C.: Theory of metamorphism of dry snow., Journal of Geophysical Research, 88, 5475–5482, https://doi.org/10.1029/JC088iC09p05475, 1983.

Comola, F., Kok, J. F., Gaume, J., Paterna, E., and Lehning, M.: Fragmentation of wind-blown snow crystals, Geophysical Research Letters, 44, 4195–4203, https://doi.org/10.1002/2017GL073039, 2017.

Dadic, R., Schneebeli, M., Bertler, N. A., Schwikowski, M., and Matzl, M.: Extreme snow metamorphism in the Allan Hills, Antarctica, as an analogue for glacial conditions with implications for stable isotope composition, Journal of Glaciology, 61, 1171–1182, https://doi.org/10.3189/2015JoG15J027, 2015.

Dansgaard, W.: Stable isotopes in precipitation, Tellus, 16, 436–468, https://doi.org/10.3402/tellusa.v16i4.8993, 1964.

Domine, F., Taillandier, A. S., and Simpson, W. R.: A parameterization of the specific surface area of seasonal snow for field use and for models of snowpack evolution, Journal of Geophysical Research: Earth Surface, 112, 1–13, https://doi.org/10.1029/2006JF000512, 2007.

Domine, F., Albert, M., Huthwelker, T., Jacobi, H.-W., Kokhanovsky, A. A., Lehning, M., Picard, G., and Simpson, W. R.: Snow physics as relevant to snow photochemistry, Tech. rep., www.atmos-chem-phys.net/8/171/2008/, 2008.

Domine, F., Taillandier, A. S., Cabanes, A., Douglas, T. A., and Sturm, M.: Three examples where the specific surface area of snow increased over time, Cryosphere, 3, 31–39, https://doi.org/10.5194/tc-3-31-2009, 2009.

Ebner, P. P., Steen-Larsen, H. C., Stenni, B., Schneebeli, M., and Steinfeld, A.: Experimental observation of transient δ18O interaction between snow and advective airflow under various temperature gradient conditions, The Cryosphere Discussions, pp. 1–36, https://doi.org/10.5194/tc-2017-16, 2017.

Faber, A. K., Vinther, B. M., Sjolte, J., and Pedersen, R. A.: How does sea ice influence δ18O of Arctic precipitation?, Atmospheric Chemistry and Physics, 17, 5865–5876, https://doi.org/10.5194/acp-17-5865-2017, 2017.

Fausto, R. S., Van As, D., Mankoff, K. D., Vandecrux, B., Citterio, M., Ahlstrøm, A. P., Andersen, S. B., Colgan, W., Karlsson, N. B., Kjeldsen, K. K., Korsgaard, N. J., Larsen, S. H., Nielsen, S., Pedersen, A. , Shields, C. L., Solgaard, A. M., and Box, J. E.: PROMICE automatic weather station data, Earth System Science Data, 80, 1–41, https://doi.org/10.22008/promice/data/aws, 2021.

Feher, R., Voiculescu, M., Chiroiu, P., and Perșoiu, A.: The stable isotope composition of hoarfrost, https://doi.org/10.1080/10256016.2021.1917567, 2021.

Flanner, M. G. and Zender, C. S.: Linking snowpack microphysics and albedo evolution, Journal of Geophysical Research Atmospheres, 111, 1–12, https://doi.org/10.1029/2005JD006834, 2006.

Flin, F. and Brzoska, J. B.: The temperature-gradient metamorphism of snow: Vapour diffusion model and application to tomographic images, Annals of Glaciology, 49, 17–21, https://doi.org/10.3189/172756408787814834, 2008.

Gallet, J. C., Domine, F., Zender, C. S., and Picard, G.: Measurement of the specific surface area of snow using infrared reflectance in an integrating sphere at 1310 and 1550 nm, Cryosphere, 3, 167–182, https://doi.org/10.5194/tc-3-167-2009, 2009.

Gallet, J. C., Domine, F., Arnaud, L., Picard, G., and Savarino, J.: Vertical profile of the specific surface area and density of the snow at Dome C and on a transect to Dumont D'Urville, Antarctica - Albedo calculations and comparison to remote sensing products, Cryosphere, 5, 631–649, https://doi.org/10.5194/tc-5-631-2011, 2011.

Gallet, J. C., Domine, F., Savarino, J., Dumont, M., and Brun, E.: The growth of sublimation crystals and surface hoar on the Antarctic plateau, Cryosphere, 8, 1205–1215, https://doi.org/10.5194/tc-8-1205-2014, 2014.

Genthon, C., Piard, L., Vignon, E., Madeleine, J. B., Casado, M., and Gallée, H.: Atmospheric moisture supersaturation in the near-surface atmosphere at Dome C, Antarctic Plateau, Atmospheric Chemistry and Physics, 17, 691–704, https://doi.org/10.5194/acp-17-691-2017, 2017.

Hachikubo, A., Yamaguchi, S., Arakawa, H., Tanikawa, T., Hori, M., Sugiura, K., Matoba, S., Niwano, M., Kuchiki, K., and Aoki, T.: Effects of temperature and grain type on time variation of snow specific surface area, Bulletin of Glaciological Research, 32, 47–53, https://doi.org/10.5331/bgr.32.47, 2014.

Hanna, E., Cropper, T. E., Jones, P. D., Scaife, A. A., and Allan, R.: Recent seasonal asymmetric changes in the NAO (a marked summer decline and increased winter variability) and associated changes in the AO and Greenland Blocking Index, International Journal of Climatology, 35, 2540–2554, https://doi.org/10.1002/joc.4157, 2015.

Holme, C., Gkinis, V., and Vinther, B. M.: Molecular diffusion of stable water isotopes in polar firn as a proxy for past temperatures, Geochimica et Cosmochimica Acta, 225, 128–145, https://doi.org/10.1016/j.gca.2018.01.015, 2018.

Hughes, A. G., Wahl, S., Jones, T. R., Zuhr, A., Hörhold, M., White, J. W. C., and Steen-Larsen, H. C.: The role of sublimation as a driver of climate signals in the water isotope content of surface snow: Laboratory and field experimental results, The Cryosphere, https://doi.org/10.5194/tc-2021-87, 2021.

Hutterli, M. A., Schneebcli, M., Freitag, J., Kipfstuhl, J., and Rothlisberger, R.: Impact of Local Insolation on Snow Metamorphism and Ice Core Records, Hokkaido University, 68, 223–232, https://doi.org/http://hdl.handle.net/2115/45450, 2009.

Johnsen, S. ., Clausen, H. B., Cuffey, K. M., Hoffmann, G., Schwander, J., and Creyts, T.: Diffusion of stable isotopes in polar firn and ice: the isotope effect in firn diffusion, Physics of Ice Core Records, pp. 121–142, 2000.

Johnsen, S. J., Dansgaard, W., and White, J. W.: The origin of Arctic precipitation under present and glacial conditions, Tellus, Series B, 41 B, 452–468, https://doi.org/10.3402/tellusb.v41i4.15100, 1989.

Klein, K.: Variability in dry Antarctic firn - Investigations on spatially distributed snow and firn samples from Dronning Maud Land, Antarctica, PhD Thesis, University of Bremen, 3, 1–15, https://doi.org/10.1016/j.cell.2009.01.043, 2014.

Kokhanovsky, A., Lamare, M., Danne, O., Brockmann, C., Dumont, M., Picard, G., Arnaud, L., Favier, V., Jourdain, B., Meur, E. L., Di Mauro, B., Aoki, T., Niwano, M., Rozanov, V., Korkin, S., Kipfstuhl, S., Freitag, J., Hoerhold, M., Zuhr, A., Vladimirova, D., Faber, A. K., Steen-Larsen, H. C., Wahl, S., Andersen, J. K., Vandecrux, B., van As, D., Mankoff, K. D., Kern, M., Zege, E., and Box, J. E.: Retrieval of snow properties from the Sentinel-3 Ocean and Land Colour Instrument, Remote Sensing, 11, https://doi.org/10.3390/rs11192280, 2019.

Laepple, T., Werner, M., and Lohmann, G.: Synchronicity of Antarctic temperatures and local solar insolation on orbital timescales, Nature, 471, 91–94, https://doi.org/10.1038/nature09825, 2011.

Laepple, T., Münch, T., Casado, M., Hoerhold, M., Landais, A., and Kipfstuhl, S.: On the similarity and apparent cycles of isotopic variations in East Antarctic snow pits, Cryosphere, 12, 169–187, https://doi.org/10.5194/tc-12-169-2018, 2018.

Landais, A., Barnola, J. M., Kawamura, K., Caillon, N., Delmotte, M., Van Ommen, T., Dreyfus, G., Jouzel, J., Masson-Delmotte, V., Minster, B., Freitag, J., Leuenberger, M., Schwander, J., Huber, C., Etheridge, D., and Morgan, V.: Firn-air δ15N in modern polar sites and glacial-interglacial ice: A model-data mismatch during glacial periods in Antarctica?, Quaternary Science Reviews, 25, 49–62, https://doi.org/10.1016/j.quascirev.2005.06.007, 2006.

Legagneux, L. and Domine, F.: A mean field model of the decrease of the specific surface area of dry snow during isothermal metamorphism, Journal of Geophysical Research: Earth Surface, 110, https://doi.org/10.1029/2004JF000181, 2005.

Legagneux, L., Cabanes, A., and Dominé, F.: Measurement of the specific surface area of 176 snow samples using methane adsorption at 77 K, Journal of Geophysical Research Atmospheres, 107, 5–1, https://doi.org/10.1029/2001JD001016, 2002.

Legagneux, L., Lauzier, T., Dominé, F., Kuhs, W. F., Heinrichs, T., and Techmer, K.: Rate of decay of specific surface area of snow during isothermal experiments and morphological changes studied by scanning electron microscopy, Canadian Journal of Physics, 81, 459–468, https://doi.org/10.1139/p03-025, 2003.

Legagneux, L., Taillandier, A. S., and Domine, F.: Grain growth theories and the isothermal evolution of the specific surface area of snow, Journal of Applied Physics, 95, 6175–6184, https://doi.org/10.1063/1.1710718, 2004.

Li, L. and Pomeroy, J. W.: Estimates of threshold wind speeds for snow transport using meteorological data, Journal of Applied Meteorology, 36, 205–213, https://doi.org/10.1175/1520-0450(1997)036<0205:EOTWSF>2.0.CO;2, 1997.

Libois, Q., Picard, G., Arnaud, L., Morin, S., and Brun, E.: Modeling the impact of snow drift on the decameter-scale variability of snow properties on the Antarctic Plateau, Journal of Geophysical Research, 119, 662–11, https://doi.org/10.1002/2014JD022361, 2014.

Libois, Q., Picard, G., Arnaud, L., Dumont, M., Lafaysse, M., Morin, S., and Lefebvre, E.: Summertime evolution of snow specific surface area close to the surface on the Antarctic Plateau, Cryosphere, 9, 2383–2398, https://doi.org/10.5194/tc-9-2383-2015, 2015.

Linow, S., Hörhold, M. W., and Freitag, J.: Grain-size evolution of polar firn: A new empirical grain growth parameterization based on X-ray microcomputer tomography measurements, Journal of Glaciology, 58, 1245–1252, https://doi.org/10.3189/2012JoG11J256, 2012.

Madsen, M. V., Steen-Larsen, H. C., Hörhold, M., Box, J., Berben, S. M., Capron, E., Faber, A. K., Hubbard, A., Jensen, M. F., Jones, T. R., Kipfstuhl, S., Koldtoft, I., Pillar, H. R., Vaughn, B. H., Vladimirova, D., and Dahl-Jensen, D.: Evidence of Isotopic Fractionation During Vapor Exchange Between the Atmosphere and the Snow Surface in Greenland, Journal of Geophysical Research: Atmospheres, 124, 2932–2945, https://doi.org/10.1029/2018JD029619, 2019.

Masson-Delmotte, V., Landais, A., Stievenard, M., Cattani, O., Falourd, S., Jouzel, J., Johnsen, S. J., Dahl-Jensen, D., Sveinsbjornsdottir, A., White, J. W., Popp, T., and Fischer, H.: Holocene climatic changes in Greenland: Different deuterium excess signals at Greenland Ice Core Project (GRIP) and NorthGRIP, Journal of Geophysical Research D: Atmospheres, 110, 1–13, https://doi.org/10.1029/2004JD005575, 2005.

Masson-Delmotte, V., Dreyfus, G., Braconnot, P., Johnsen, S., Jouzel, J., Kageyama, M., Landais, A., Loutre, M.-F., Nouet, J., Parrenin, F., Raynaud, D., Stenni, B., and Tuenter, E.: Climate of the Past Past temperature reconstructions from deep ice cores: relevance for future climate change, Tech. rep., www.clim-past.net/2/145/2006/, 2006.

Merlivat, L. and Jouzel, J.: Global climatic interpretation of the deuterium-oxygen 16 relationship for precipitation., Journal of Geophysical Research, 84, 5029–5033, https://doi.org/10.1029/JC084iC08p05029, 1979.

Neumann, T. A. and Waddington, E. D.: Effects of firn ventilation on isotopic exchange, Journal of Glaciology, 50, 183–194, https://www.cambridge.org/core., 2004.

Neumann, T. A., Albert, M. R., Engel, C., Courville, Z., and Perron, F.: Sublimation rate and the mass-transfer coefficient for snow sublimation, International Journal of Heat and Mass Transfer, 52, 309–315, https://doi.org/10.1016/j.ijheatmasstransfer.2008.06.003, 2009.

Picard, G., Royer, A., Arnaud, L., and Fily, M.: Influence of meter-scale wind-formed features on the variability of the microwave brightness temperature around Dome C in Antarctica, Cryosphere, 8, 1105–1119, https://doi.org/10.5194/tc-8-1105-2014, 2014.

Picard, G., Arnaud, L., Caneill, R., Lefebvre, E., and Lamare, M.: Observation of the process of snow accumulation on the Antarctic Plateau by time lapse laser scanning, Cryosphere, 13, 1983–1999, https://doi.org/10.5194/tc-13-1983-2019, 2019.

Pinzer, B. and Schneebeli, M.: Temperature gradient metamorphism is not a classical coarsening process, ISSW 09 - International Snow Science Workshop, Proceedings, pp. 58–61, 2009a.

Pinzer, B. R. and Schneebeli, M.: Snow metamorphism under alternating temperature gradients: Morphology and recrystallization in surface snow, Geophysical Research Letters, 36, 10–13, https://doi.org/10.1029/2009GL039618, 2009b.

Pinzer, B. R., Schneebeli, M., and Kaempfer, T. U.: Vapor flux and recrystallization during dry snow metamorphism under a steady temperature gradient as observed by time-lapse micro-tomography, Cryosphere, 6, 1141–1155, https://doi.org/10.5194/tc-6-1141-2012, 2012.

Ritter, F., Christian Steen-Larsen, H., Werner, M., Masson-Delmotte, V., Orsi, A., Behrens, M., Birnbaum, G., Freitag, J., Risi, C., and Kipfstuhl, S.: Isotopic exchange on the diurnal scale between near-surface snow and lower atmospheric water vapor at Kohnen station, East Antarctica, Cryosphere, 10, 1647–1663, https://doi.org/10.5194/tc-10-1647-2016, 2016.

Schaller, C. F., Freitag, J., and Eisen, O.: Critical porosity of gas enclosure in polar firn independent of climate, Climate of the Past, 13, 1685–1693, https://doi.org/10.5194/cp-13-1685-2017, 2017.

Sime, L. C., Risi, C., Tindall, J. C., Sjolte, J., Wolff, E. W., Masson-delmotte, V., and Capron, E.: Warm climate isotopic simulations : what do we learn about interglacial signals in Greenland ice cores ?, Quaternary Science Reviews, 67, 59–80, https://doi.org/10.1016/j.quascirev.2013.01.009, 2013.

Sodemann, H., Masson-Delmotte, V., Schwierz, C., Vinther, B. M., and Wernli, H.: Interannual variability of Greenland winter precipitation sources: 2. Effects of North Atlantic Oscillation variability on stable isotopes in precipitation, Journal of Geophysical Research Atmospheres, 113, 1–21, https://doi.org/10.1029/2007JD009416, 2008.

Sokratov, S. A. and Golubev, V. N.: Snow isotopic content change by sublimation, Journal of Glaciology, 55, 823–828, https://doi.org/10.3189/002214309790152456, 2009.

Steen-Larsen, H. C., Sveinbjörnsdottir, A. E., Peters, A. J., Masson-Delmotte, V., Guishard, M. P., Hsiao, G., Jouzel, J., Noone, D., Warren, J. K., and White, J. W.: Climatic controls on water vapor deuterium excess in the marine boundary layer of the North Atlantic based on 500 days of in situ, continuous measurements, Atmospheric Chemistry and Physics, 14, 7741–7756, https://doi.org/10.5194/acp-14-7741-2014, 2014.

Stenni, B., Scarchilli, C., Masson-Delmotte, V., Schlosser, E., Ciardini, V., Dreossi, G., Grigioni, P., Bonazza, M., Cagnati, A., Karlicek, D., Risi, C., Udisti, R., and Valt, M.: Three-year monitoring of stable isotopes of precipitation at Concordia Station, East Antarctica, Cryosphere, 10, 2415–2428, https://doi.org/10.5194/tc-10-2415-2016, 2016.

Taillandier, A. S., Domine, F., Simpson, W. R., Sturm, M., and Douglas, T. A.: Rate of decrease of the specific surface area of dry snow: Isothermal and temperature gradient conditions, Journal of Geophysical Research: Earth Surface, 112, 1–13, https://doi.org/10.1029/2006JF000514, 2007.

Touzeau, A., Landais, A., Stenni, B., Uemura, R., Fukui, K., Fujita, S., Guilbaud, S., Ekaykin, A., Casado, M., Barkan, E., Luz, B., Magand, O., Teste, G., Le Meur, E., Baroni, M., Savarino, J., Bourgeois, I., and Risi, C.: Acquisition of isotopic composition for surface snow in East Antarctica and the links to climatic parameters, Cryosphere, 10, 837–852, https://doi.org/10.5194/tc-10-837-2016, 2016.

Touzeau, A., Landais, A., Morin, S., Arnaud, L., and Picard, G.: Numerical experiments on vapor diffusion in polar snow and firn and its impact on isotopes using the multi-layer energy balance model Crocus in SURFEX v8.0, Geoscientific Model Development, 11, 2393–2418, https://doi.org/10.5194/gmd-11-2393-2018, 2018.

Town, M. S., Waddington, E. D., Walden, V. P., and Warren, S. G.: Temperatures, heating rates and vapour pressures in near-surface snow at the South Pole, Tech. Rep. 186, 2008.

Van Geldern, R. and Barth, J. A.: Optimization of instrument setup and post-run corrections for oxygen and hydrogen stable isotope measurements of water by isotope ratio infrared spectroscopy (IRIS), Limnology and Oceanography: Methods, 10, 1024–1036, https://doi.org/10.4319/lom.2012.10.1024, 2012.

Vimeux, F., Masson, V., Jouzel, J., Stievenard, M., and Petit, J. R.: Glacial-interglacial changes in ocean surface conditions in the Southern Hemisphere, Nature, 398, 410–413, 1999.

Vimeux, F., Masson, V., Delaygue, G., Jouzel, J., Petit, J. R., and Stievenard, M.: A 420,000 year deuterium excess record from East Antarctica: Information on past changes in the origin of precipitation at Vostok, Journal of Geophysical Research Atmospheres, 106, 31 863–31 873, https://doi.org/10.1029/2001JD900076, 2001.

Vinther, B. M., Buchardt, S., Clausen, H., Dahl-Jensen, D., Johnsen, S., Fisher, D., Koerner, R., Raynaud, D., Lipenkov, V., Andersen, K., Blunier, T., Rasmussen, S., Steffensen, J., and Svensson, A.: Holocene thinning of the Greenland ice sheet, Nature, 461, 385–388, 2009.

Wahl, S., Steen-Larsen, H. C., and Reuder, J.: Quantifying the Stable Water Isotopologue Exchange between Snow Surface and Lower Atmosphere by Direct Flux Measurements, Journal of Geophysical Research: Atmospheres, https://doi.org/10.1029/2020jd034400, 2021.

Zuanon, N.: IceCube, a portable and reliable instrument for snow specific surface area measurement in the field, International Snow Science Workshop, pp. 1020–1023, www.A2PhotonicSensors.com, 2013.

Zuhr, A. M., Münch, T., Steen-Larsen, H. C., Hörhold, M., and Laepple, T.: Local-scale deposition of surface snow on the Greenland ice sheet, The Cryosphere, 15, 4873–4900, https://doi.org/10.5194/tc-15-4873-2021, 2021.